A G M A
P-299.06—A

GEAR NOISE -
THE GENERATION OF ROTATIONAL HARMONIC FREQUENCIES
IN MARINE PROPULSION GEARS

BY

George W. Nagorny - Head, Main Propulsion and Ship Silencing Section

Richard A. Stutchfield - Senior Project Engineer

from

Naval Ship Systems Engineering Station Headquarters

Presented at the Fall Technical Meeting of the
American Gear Manufacturers Association
Four Seasons Hotel
Toronto, Canada
October 10-14, 1981

GEAR NOISE

THE GENERATION OF ROTATIONAL HARMONIC FREQUENCIES IN MARINE PROPULSION GEARS

INTRODUCTION

Much has been written on the factors that are involved in the generation of gear noise. It has not been until recently, however, that there has been much written about the generation of the rotational harmonics (sidebands) that surround the gear tooth meshing frequency. During recent testing of large marine propulsion gears at Naval Ship Systems Engineering Station Headquarters (NAVSSES) [formerly Naval Ship Engineering Center, Philadelphia (NAVSEC) and before that, Naval Boiler and Turbine Laboratory (NBTL)], it became evident to the U.S. Navy that these rotational harmonics were an extremely important part of the gear noise picture. The complex and seemingly random nature of this rotational harmonic structure around gear tooth meshing frequency made an analytical method of analysis the only possible solution.

At the same time the U.S. Navy was conducting these tests, Bolt, Beranek and Newman (BBN) in Cambridge, MA was developing, from first principles, a gear noise prediction model that would account for all of the gear design parameters, machining errors, and shafting dynamics. Therefore, the U.S. Navy and BBN decided to work together to validate this gear noise prediction model. It is the purpose of the paper to present information developed from the testing, gear measurements and analytical work done in the area of rotational harmonic generation.

TEST FACILITY AND EQUIPMENT

The test facility used for this test was an open loop, double reduction, double input, locked-train marine propulsion plant. An isometric of such a locked-train gear is shown in Fig. 1. Due to the nature of this gear test, actual test details cannot be given. However, it is sufficient to say that the test unit is in the realm of typical Navy-sized, main propulsion units.

The test gear unit was instrumented with piezoelectric accelerometers for recording of structureborne vibrations. These accelerometers were mounted on the gear casing, foundation, and selective gear element bearing caps. There were capabilities for on-line data analysis as well as recording data for later analyses. The vibration data used for the study of the rotational harmonics (sidebands) in this paper was data recorded on the gear element bearing caps.

In order to provide accurate and repeatable gear error data needed for gear noise prediction model use and for study of the rotational harmonic structure in the vibration data, improved methods of gear error measurement over those available at NAVSSES were needed. A new Gear Metrology Facility was constructed and equipped at NAVSSES to meet these requirements. This new facility consists of a 32' x 40', 16'-high modular room, climate controlled to $20^{o}C \pm 1^{o}C$ and $40\% \pm 5\%$ relative humidity. Fig. 2 shows some of the gear error measurement and analysis equipment contained within the facility: a MAAG SP-160 gear tooth profile and helix angle measuring machine (mounted on 1.5 Hz air mounts for vibration isolation; and with ES-415 control unit) capable of measuring a gear up to 63" diameter, 47" face width, and weighing over 15,000 lbs; an HP-9845T computer which

allows the data (digital) to be processed in other formats or onto digital tape; a MAAG ES-401 portable gear tooth spacing measurement machine and control unit which can provide a diagram or printed tape of the spacing data, or be linked to the computer for putting data onto digital tape.

BBN GEAR NOISE PREDICTION MODEL

The BBN gear noise prediction model that we have been working on with BBN to validate is thoroughly described in [1][1] and [2]. The foundation for this model is that the excitation for gear vibration comes from the static transmission error (STE) between the meshing gear teeth on a gear helix.

The STE consists of two basic components, a mean component and a random component. The mean component in turn consists of three parts: a "load-dependent part caused by elastic tooth deformation, plus components arising from the mean deviation of the unloaded tooth surfaces of each of the meshing gear helices from perfect involute surfaces. The random contributions from each meshing gear helix arise from differences between the mean tooth-face surface for that helix and the actual surfaces of the individual teeth of that helix" [3].

The mean component of the STE is directly related to the vibration at the gear meshing frequency fundamental and harmonics. The contribution of the random component of the STE is seen in the rotational frequency fundamental and harmonics.

[1] Bracketed numbers refer to references at the end of the text.

Although we will touch upon the mean component of the STE, the emphasis of the present paper is on the random component of the STE and on the rotational frequency harmonics occurring in the vicinity of the gear meshing frequency fundamental. These "spikes" near the gear mesh frequency in the vibration spectra are often referred to as "sidebands". The dictionary [4] definition of the term "sideband" is as follows: "The band of (radio) frequencies on either side of the carrier frequency produced by modulation." In [5], a case is made that these "spikes" are in fact sidebands: i.e., frequencies resulting from modulation of the mesh frequency. For the purposes of this paper, we will assume {following the analysis of Dr. Mark in [1]} that what we call the higher order rotational harmonics are in fact harmonics generated by the random component of the STE.

Fig. 3 shows the contributions to the noise spectrum from various types of tooth errors from a single gear or pinion. The two heavy lines represent the gear mesh fundamental and first harmonic, and their amplitudes are determined by the mean component of the STE. The U.S. Navy (1) is developing the means to determine the tooth elastic deformations and (2) has the means to measure the involute modifications at the NAVSSES Gear Metrology Facility. Capabilities in (1) and (2) are needed to determine the mean component of the STE. Proof that the random components of the STE do not contribute to the tooth meshing harmonics is given in [6].

Note that the remaining noise "spikes" harmonics are due to the random component of the STE.

Before continuing, it should be noted that the multiplicity of teeth in the meshing zone results in an attenuation of the RMS errors in a characteristic manner which is specific to, (1) the "type of error," and (2) the specific gear design.

The standard tooth error measurements are taken and are analyzed using Legendre polynomials which provide us with the specific "type of error." The Legendre polynomials which Dr. Mark selected [2], lead to a mathematical representation of the tooth errors which has a physical meaning to those in the gear field. For example, when one evaluates the Legendre polynomial with its indices "k" and "ℓ" we have the following:

$k = 0, \ell = 0$	yield the tooth spacing error,
$k = 0, \ell = 1$	pure involute slope error,
$k = 1, \ell = 0$	pure lead mismatch error,
$k = 0, \ell = 2$	pure involute fullness error, and
$k = 1, \ell = 1$	combined lead mismatch-involute slope error

Returning to Fig. 3, note that the tooth spacing errors are the only errors which contribute to the low-order rotational harmonics. Also note that tooth-to-tooth errors other than tooth spacing errors contribute to the rotational harmonics which occur immediately to the left and to the right of the tooth mesh harmonics. All types of tooth-to-tooth errors contribute to the other higher-order rotational harmonics.

To explain the contributions noted above, we must look at the mesh transfer functions. The mesh transfer functions are dependent on design and these functions are what determine the attenuating effects (resulting from the multiplicity of teeth in the meshing zone) on the "Lengendre polynomial defined error"; e.g., the $k = 0$, $\ell = 0$ which is the tooth spacing error.

If we make a discrete Fourier analysis of the accumulated tooth spacing error data we will find the error RMS amplitude of all harmonic orders from 1 to N-1 (where N is equal to the number of teeth on the gear). The RMS amplitude of the 1 and N-1 harmonic orders are equal as are the 2 and N-2, 3 and N-3, etc., harmonic orders. It turns out that the RMS amplitudes of the harmonic orders between 0 and N (from 1 to N-1) are the same as those between N and 2N {from N + (1) to N + (N-1)} and between all other consecutive harmonics of mesh: between (h)N and (h + 1)N, where h = the lower of two harmonics in question.

Fig. 4 is the mesh transfer function for the tooth spacing error. Note that at the lower harmonic numbers there is zero (10^{o}) attenuation. When the discrete Fourier spectrum of the tooth spacing error is properly normalized and multiplied by the mesh transfer function, the result yields the mesh-attenuated error spectrum for tooth spacing. This result is the STE contribution of the tooth spacing error on the noise.

A similar process must take place for each of the other "Legendre polynomial defined errors"; e.g., the k = 0, ℓ = 1 involute slope error; k = 1, ℓ = 0 lead mismatch error; k = 1, ℓ = 1 combined lead mismatch-involute slope error, etc. The mesh transfer functions for these 3 Legendre polynomial errors are shown in Figs. 5, 6 and 7 respectively. Note that there is anywhere from 10 (10^{1}) to 1000 (10^{3}) times attenuation at the lower order rotational harmonics. All mesh transfer functions are dependent only on the gear tooth design and hence independent of the tooth error system.

GEAR ERROR

The gear noise prediction model requires that a tooth surface representation of the errors be provided. Fig. 8 is a computer plot made from measured data taken on one tooth indicating the kind of data one might take. The mathematical analyses procedures used are beyond this paper. The mean error for all the teeth would be found, as well as the values for the difference between each individual tooth error and the mean tooth error. It is the amplitude from discrete Fourier analysis of these differences which will be responsible for the rotational harmonic frequencies. This then, is why variability in manufacture must be minimized to reduce the noise from the rotational harmonic frequencies!

The following section shows some measurements of this variability which we have observed on some high-speed gear elements.

Helix Angle Error

Fig. 9 shows helix angle error measurements taken on 2 different teeth at 3 different radii on one helix of a double-helical, hobbed and shaved, high speed pinion. Every measurement shows some random bumps with heights of about 0.0001 inch. Note that on tooth no. 1 the helix angle slope (mismatch) error over about 4-1/2 inch of the 5-3/8 inch face width varies from 0.0001 inch at R2 to a maximum of 0.0003 inch at the R1 radius. Fig. 10 shows helix angle error measurements on the same hobbed and shaved pinion taken at the pitchline on 4 teeth around the pinion, with random bumps, and with the slope error varying from 0 to 0.0002 inch.

Helix error measurements taken on a MAAG-ground, single-helical, high speed pinion are shown in Figs. 11 and 12. Note that the diagram

lengths are Xerox-reduced and that the actual face width is 10-5/8 inch. Fig. 11 shows that the lead modification for a given radial position is slightly different than that at the other two radial positions on a given tooth. This difference appears to be a characteristic of the grinding process used and results in a 0.00015 inch greater lead fullness at the R2 radius than at the R1 radius. There is some waviness present but it is of very short wavelength and only about 0.00005 inch amplitude. Fig. 12 shows that the variability of the lead modification around the gear is less than 0.0001 inch for the forward half of the face and up to about 0.0002 inch for the remainder of face width.

On a per inch face width basis, the ground gear has about one-third the lead variability of the hobbed and shaved gear. The relationship between lead variability and noise mentioned previously in the gear noise model will be shown vividly in the gear noise section.

Profile Error

Fig. 13 shows profile error measurements taken on two teeth at 3 different axial positions on the same teeth used for demonstrating hobbed and shaved lead variability. The profiles have a slight fullness and some random bumps along the surface. The profile taken at the forward end is seen to have 2 large bumps on each tooth (near the pitch diameter), with the respective bump height different on the two teeth shown. Fig. 14 shows profile error measurements on the same hobbed and shaved pinion taken at the tooth center on 4 teeth around the pinion, with a composite of these 4 measurements which shows a variability of about 0.00015 inch.

Profile error measurements taken on the same MAAG-ground, single-helical, high speed pinion teeth used for demonstrating MAAG-ground lead

variability are shown in Figs. 15 and 16. Fig. 15 shows that the profiles along a tooth are very smooth and uniform. Fig. 16 shows that the profile around the pinion is virtually identical in the unmodified portion and has a variability of less than 0.0001 inch in the modified areas.

The random bumps on the hobbed and shaved profiles, and the variability in the modified areas of the MAAG-ground profiles will each be of sufficient magnitude to contribute to the rotational harmonics of the respective gears. However, in comparison to the contribution from the variability in hobbed and shaved gear helix angle errors, the contribution from these profile variations should be minor.

Tooth Spacing Error

Tooth spacing error measurements have been used extensively for many years for tracking the accuracy of gears from the wormwheel of the master hobber, through to the production gear. Tooth spacing error is in fact a measure of variation (in spacing), and therefore contributes to the rotational harmonics. The RMS amplitude of the 1st and N-1 {and also the N + (1) and N + (N-1), 2N + (1) and 2N + (N-1), etc., as noted above} harmonic numbers from the discrete Fourier analysis of the tooth spacing error are (identical and) usually the highest amplitudes of all the tooth spacing error harmonics. As discussed above, the tooth spacing mesh transfer function (Fig. 4) causes the mesh-attenuated amplitude of the N-1 and N + 1 harmonics to be reduced so as to be very substantially reduced. Since in most cases the level of vibration at the N-1 and N + 1 harmonics for high accuracy marine gears is higher than the other-high order rotational harmonics, the tooth spacing contribution is obviously not domineering. The entire tooth surface representation for every tooth

must be used in establishing the tooth spacing information needed for the model's Legendre polynomial analysis. No further discussion will be made in this paper on the tooth spacing error contribution.

NOISE DATA

Piezoelectric accelerometers on the reduction gear element bearing caps inside the gear casing allowed for a more direct look at the sources of the gear noise.

In order to study the rotational frequency harmonic activity, a method was developed to permit the closely-spaced frequency components in the spectra around gear tooth meshing frequency (as shown for a typical spectra in the upper half of Fig. 17) to be expanded by "translation" (as shown in the lower half of Fig. 17). This translation enabled gear tooth meshing frequency to be separated from the closely-spaced rotational harmonic structure. Unfortunately, this preliminary technique was sensitive to relatively small machinery speed changes which made it difficult to discern the tooth meshing frequency from that of the higher order rotational frequency harmonics. (The tooth meshing frequency and adjacent rotational harmonics would smear as the speed changed.) However, this difficulty was overcome with the development of another technique that would "track" the tooth meshing frequency, as well as translate. This now allowed for positive identification of the discrete tooth meshing frequency and the adjacent rotational frequency harmonics.

Once positive identification was achieved, it could be said with authority that the "hump" callled meshing frequency seen in the spectra at the top of Fig. 17 actually consisted of a discrete gear meshing frequency component surrounded by discrete components spaced at rotational

harmonic frequency as seen in the lower half of (Fig. 17). It is clearly evident that the amplitudes of these higher-order harmonics of rotational frequency are significant relative to the amplitudes of mesh, and hence are an important contribution to overall noise.

Additional study of the translated spectrum around mesh disclosed several characteristics of the rotational harmonic structure that suggested a very complex and random behavior. First, when observing the translated spectrum for a particular gear element in real time at seemingly steady state conditions, the rotational harmonic structure changed dramatically. Second, gear elements of the same design, manufactured on the same machine with identical accuracy limits were tested under identical conditions, and the vibration spectra showed that the rotational harmonic frequency structures for the elements were different. It was part of this test program to investigate these phenomenon. From the preliminary results of this investigation, the following statements can be made:

1. <u>The higher-order rotational harmonic structure is greatly affected by the resonant nature of a marine propulsion gear set</u>.

During the early part of this investigation, it was found that when several mesh translations of a particular gear element were taken at different times (and seemingly identical conditions), the rotational harmonic structure was different. Additionally, when the translated spectrum for a particular gear element was observed in real time, the rotational harmonic structure appeared to be unstable. Great effort was then expended to control the test operating conditions in order to observe their effect on

the rotational harmonic structure. Load, speed, and oil temperature were varied independently. It was found that the only operating condition that greatly affected the rotational harmonic structure was speed. When great care was given to obtaining identical speeds, the rotational harmonic structure for a particular gear element was repeatable.

The next step of the investigation was to determine why the rotational harmonic structure was sensitive to variation in speed. Fig. 18 shows plots of discrete mesh frequency, a prominent discrete high-order rotational frequency harmonic near mesh, and speed, all versus time (over a 5 minute period). As the speed fluctuates with time, it can be seen that the amplitude of the discrete mesh frequency and the amplitude of the rotational frequency harmonic vary. The most significant feature of these plots is that each time the speed drops below the reference speed line, the discrete mesh frequency amplitude increases and the rotational frequency harmonic amplitude drops. Additionally, as soon as the speed rises above the speed reference line, the discrete mesh frequency and rotational harmonic amplitudes return to their original values. This behavior is characteristic of local resonance. Through similar "tracking" of all the prominent rotational harmonic frequencies around the discrete mesh frequency, it has been determined that this amplitude variation, previously thought to be some kind of instability, is mainly a result of the interplay between these excitations and local resonances. By the nature of their construction, marine propulsion gears are large, hollow cylinders with little damping, and will act as excellent amplifiers for these resonance responses.

2. Higher-order rotational harmonic structure is relatively insensitive to load variation.

During the investigation of the effects of operating conditions on rotational harmonic structure, load was one of the conditions controlled. It was found that small variations of load (± 2%) did not affect the rotational harmonic structure. It later became of interest to investigate the effects of gross changes in load on the rotational harmonic structure. During the tests, great effort was expanded to obtain identical speed conditions. Fig. 19 shows the translated mesh of a test gear element at one speed with four different load conditions (100%, 75%, 50% and 25% torque conditions). The rotational harmonic structure remains relatively constant as the load is lowered from 100 through 75 to 50 percent. At the 25 percent load condition, the rotational harmonic structure seems to change. However, at this lightly-loaded condition, the elements are not running at the same stable positions in their bearings, and the results would be expected to be different.

3. Each gear element has its own individual rotational harmonic structure.

As discussed previously in this paper, the higher order rotational harmonics are generated by the variations of the individual gear tooth surfaces from the mean tooth surface for that helix. Therefore, even though two gear elements have identical gear design parameters, are manufactured to high quality standards on the same machine, and are run at identical conditions, they can have different rotational harmonic structures. Fig. 20 shows the rotational harmonic structure for two

"identical" input pinions. It can be seen that the rotational harmonic structure is different. Although a complete set of gear error measurements has not yet been taken for these input pinions, cursory measurements indicate strikingly different error patterns which in turn will lead to different rotational harmonic structures.

Since it is the variability of the individual gear tooth surfaces from the mean tooth surface for that helix that generates the rotational harmonics, the reduction of that variability will reduce the amplitude of the rotational harmonics. Rotational harmonics are partially a function of the machining process. During the tests at NAVSSES, two different machining processes were used for test gear elements: (1) hobbed and shaved and (2) ground. Figs. 10 and 14 show typical error measurements for the hobbed and shaved gears that were tested with variability evident in the measurements. Figs. 12 and 16 show typical error measurements for the ground gears that were tested, and these measurements show much less variability. These differences in variation should be evident in the vibration data for the rotational harmonic structures for the different gear elements. Fig. 21 shows the vibratory rotational harmonic structure for both a hobbed and shaved gear, and a ground gear. As expected from the gear error measurement data noted earlier, the amplitude of the rotational harmonics surrounding the discrete mesh frequency are significantly lower on the ground gear, obviously from the smaller error variation.

4. Gear rim stiffness variations significantly affect rotational harmonics.

It has been found that "lightening holes" and stiffening members

in the gear webs can change the effective gear rim stiffness. The rotational harmonic structure will reflect this because the variation in gear rim stiffness will affect the elastic deflections of the individual gear teeth. Fig. 22 shows vibration data on the rotational harmonic structure of two different test gear elements. The upper translation shows the rotational harmonic structure for a gear having 3 stiffening members spaced at 120° intervals around the gear. It can be seen that multiples of the number of stiffeners are the predominent rotational harmonics ($\pm$ 3, $\pm$ 6). The lower translation on Fig. 22 shows the rotational harmonic structure for a gear having 6 stiffening numbers spaced at 60° intervals around the gear. Once again it is multiples of the number of stiffening members that are the predominent rotational harmonic ($\pm$ 6, $\pm$ 12). Cases where stiffeners are present and yet rotational harmonics due to the stiffeners are not dominant result mainly due to the local resonant phenomena detailed earlier in this paper.

CONCLUSIONS

Every gear element has its own unique gear error system and hence vibratory characteristics.

The variability of the lead and profile errors on a given gear helix from the two different gear machining processes examined were different. Hobbed and shaved gears showed greater variability in these errors than MAAG-ground gears.

Gears with higher variability in profile and lead errors show more significant vibration amplitude for the high-order harmonics of rotational frequency.

The resonant nature of large marine gears makes the vibratory structure of the higher-order rotational harmonics very sensitive to small speed changes. Changes in load over a wide range does not appear to have a significant effect on this structure.

The variability of effective rim stiffness resulting from the discontinuities in the structure supporting the gear teeth, such as with multiple web stiffeners, can result in significant vibration from this source.

SUMMARY

This paper discussed qualitatively the relationship between variability of tooth errors and the generation of vibration at rotational frequency harmonics. Particular emphasis was given to the variability of profile and lead errors, and the effect of this variability on the higher-order rotational frequency harmonics.

The gear noise prediction model developed by Dr. William D. Mark provides the analytical tool needed to quantify the effects of the tooth error (variability) and to quantify the effects of the tooth design and shafting dynamic design on generation of the entire vibration spectrum.

ACKNOWLEDGEMENTS

We are indebted to Stephen M. Blazek, Sigitas Leimonas, and Stephen G. Wieczorek at the Naval Sea Systems Command for their support through the Gear RDT&E Program which made this paper possible. We also wish to thank Dr. William D. Mark at BBN for being available as a resource person on the technical aspects of the gear noise prediction model and Dr. Fred A. Kern at BBN for his contributions to the design of the instrumentation and the development of the test program. At NAVSSES there

were many who assisted, but the following persons contributed most significantly: Joseph J. DeLucia for gear metrology, Joseph W. Fedena for vibration acquisition and analysis, Leonard J. Wolkowicz for graphics, Henry G. Hamre for test operation and Marion R. Matteo for typing of the paper.

We are grateful to the persons and organizations who granted permission for the use of the Figures noted:

Fig. 2 is taken from drawing (g) of Chapter IX written by Harold W. Semar in Marine Engineering 1971 edited by Roy L. Harrington and published by The Society of Naval Architects and Marine Engineers.

Figs. 3 through 7 are from a presentation by Dr. William D. Mark, BBN, at NAVSSES on 11 and 12 June 1980.

REFERENCES

1. W. D. Mark, "Analysis of the Vibratory Excitation of Gear Systems: Basic Theory," J. Acoust. Soc. Am., Vol. 63, No. 5, ppg 1409-1430, May 1978

2. W. D. Mark, "Analysis of the Vibratory Excitation of Gear Systems II: Tooth Error Representations, Approximations, and Application," J. Acoust. Soc. Am., Vol. 66, No. 6, ppg 1758-1787, Dec 1979

3. Taken from ppg 1423 of reference 1

4. Webster's Third New International Dictionary

5. A. M. Thomson, "Fourier Analysis of Gear Errors," presented at NELEX 80 International Metrology Conference at National Engineering Laboratory East Kilbride, Scotland

6. Appendix H on ppg 1429 of reference 1

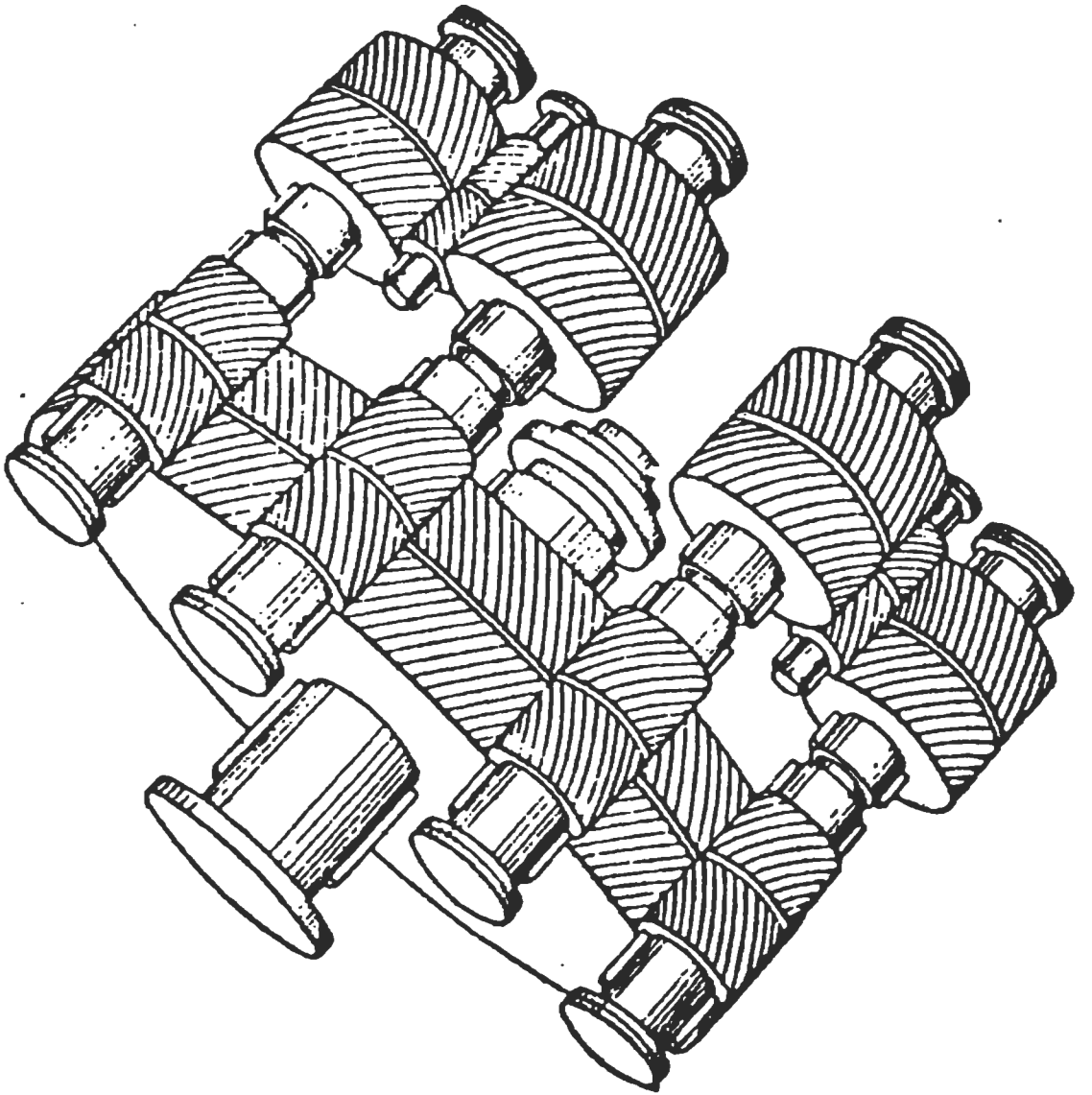

Double reduction, double input, locked train gear

(From Chapter IX, Figure 2 of Marine Engineering, 1971)

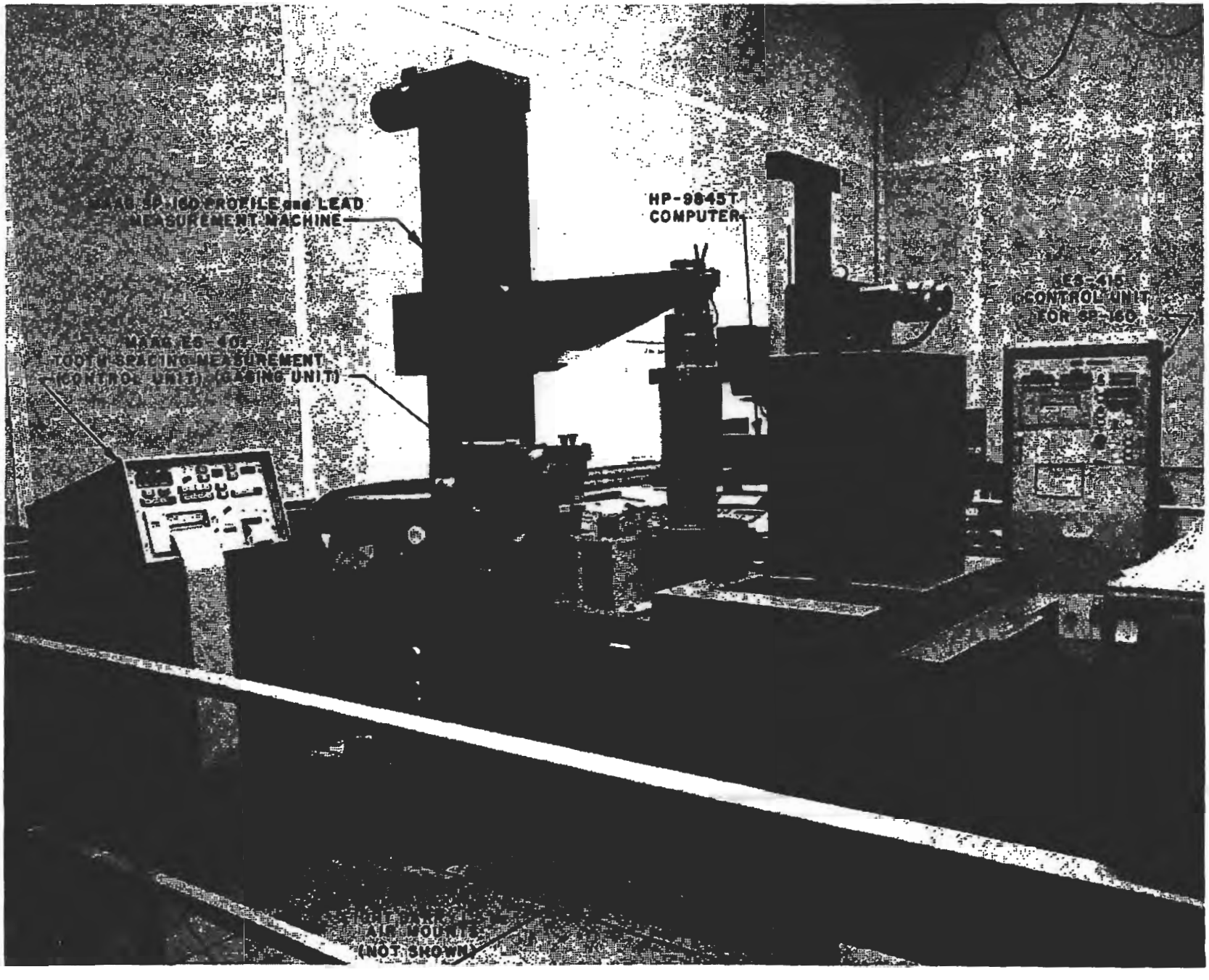
HP-9845T
COMPUTER

CONTRIBUTIONS TO NOISE SPECTRUM FROM VARIOUS TYPES OF TOOTH ERRORS FROM A SINGLE GEAR OR PINION

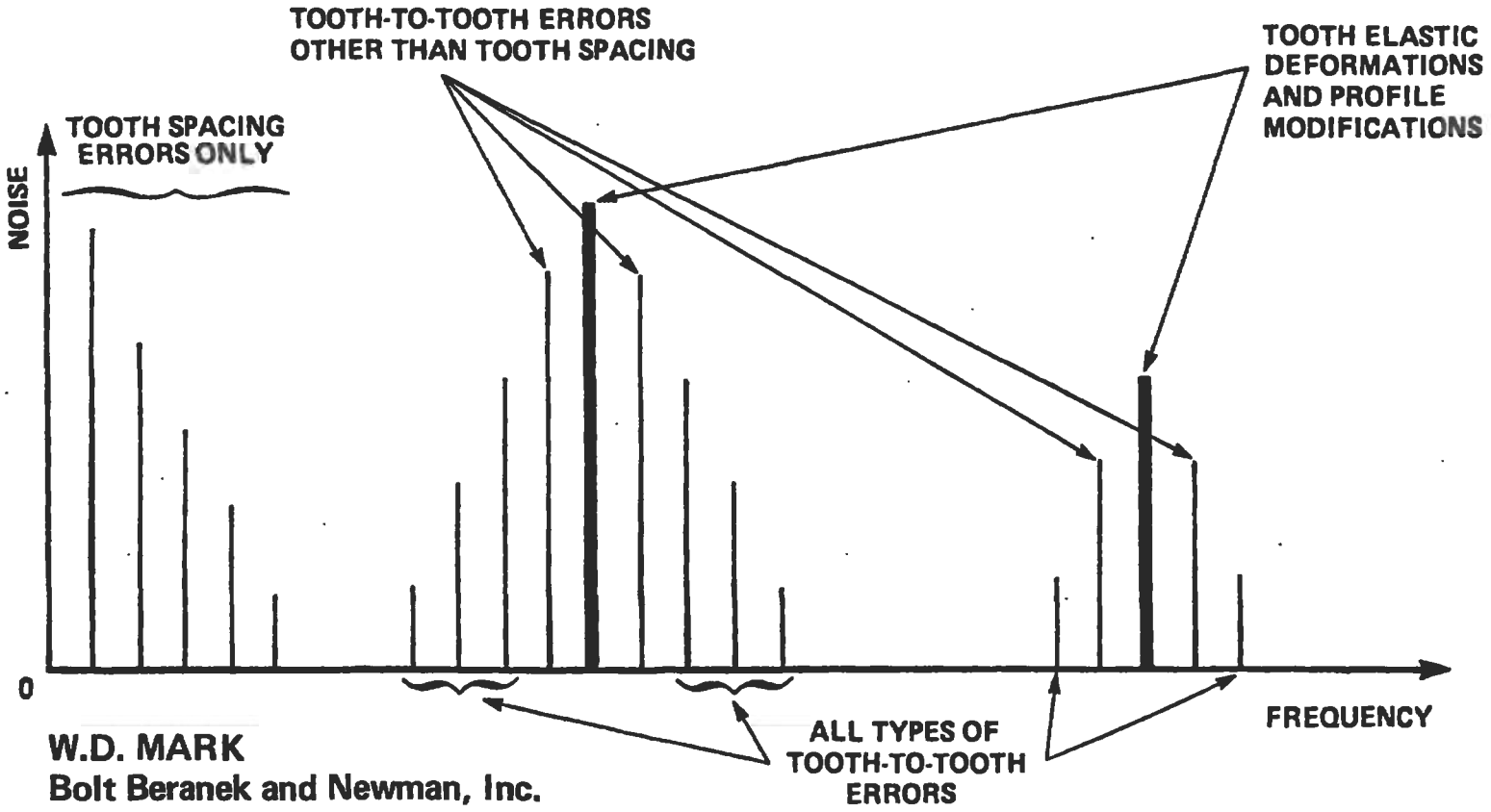

(From Presentation by W. D. Mark on 11,12 June 1980 at NAVSSES)

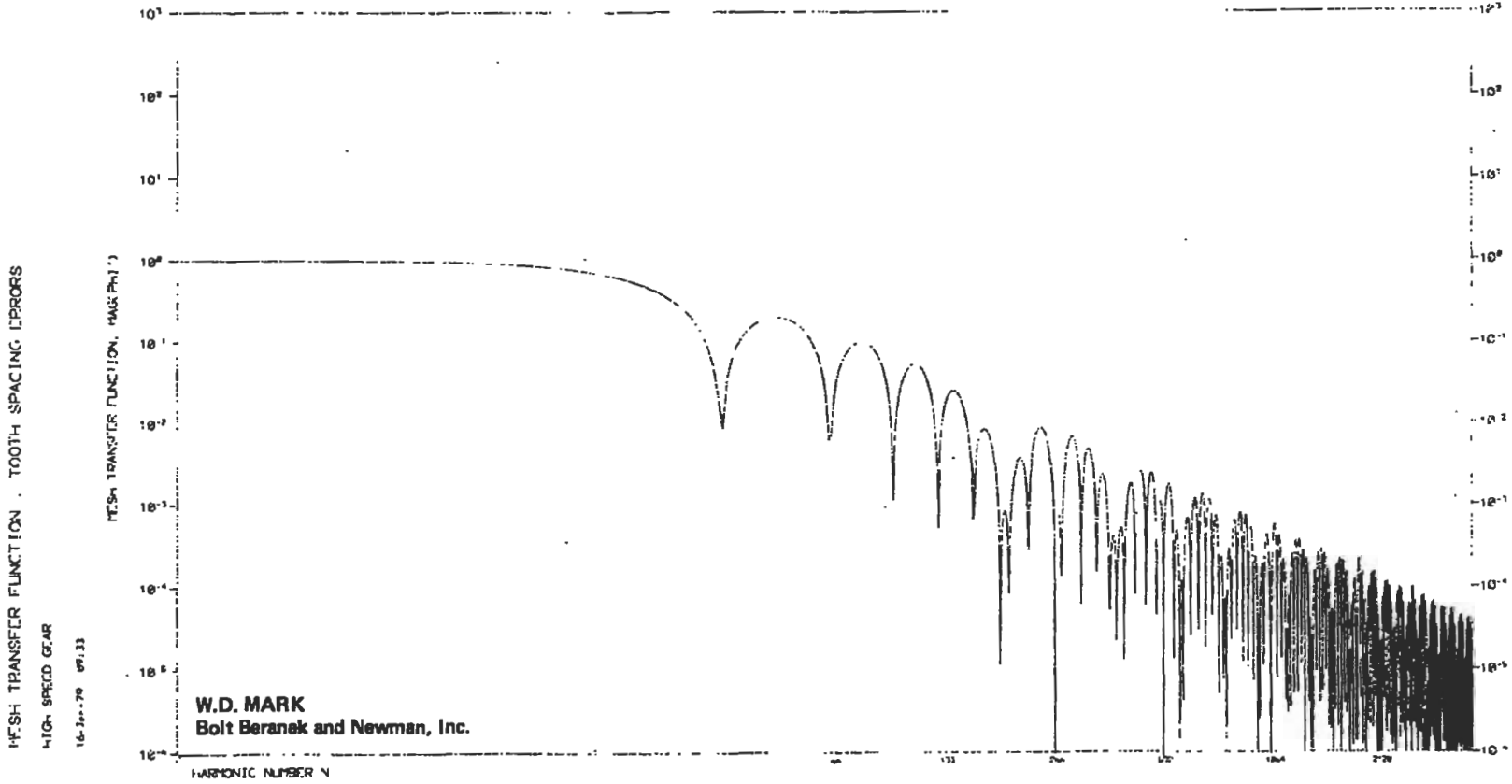

(From Presentation by W. D. Mark on 11,12 June 1980 at NAVSSES)

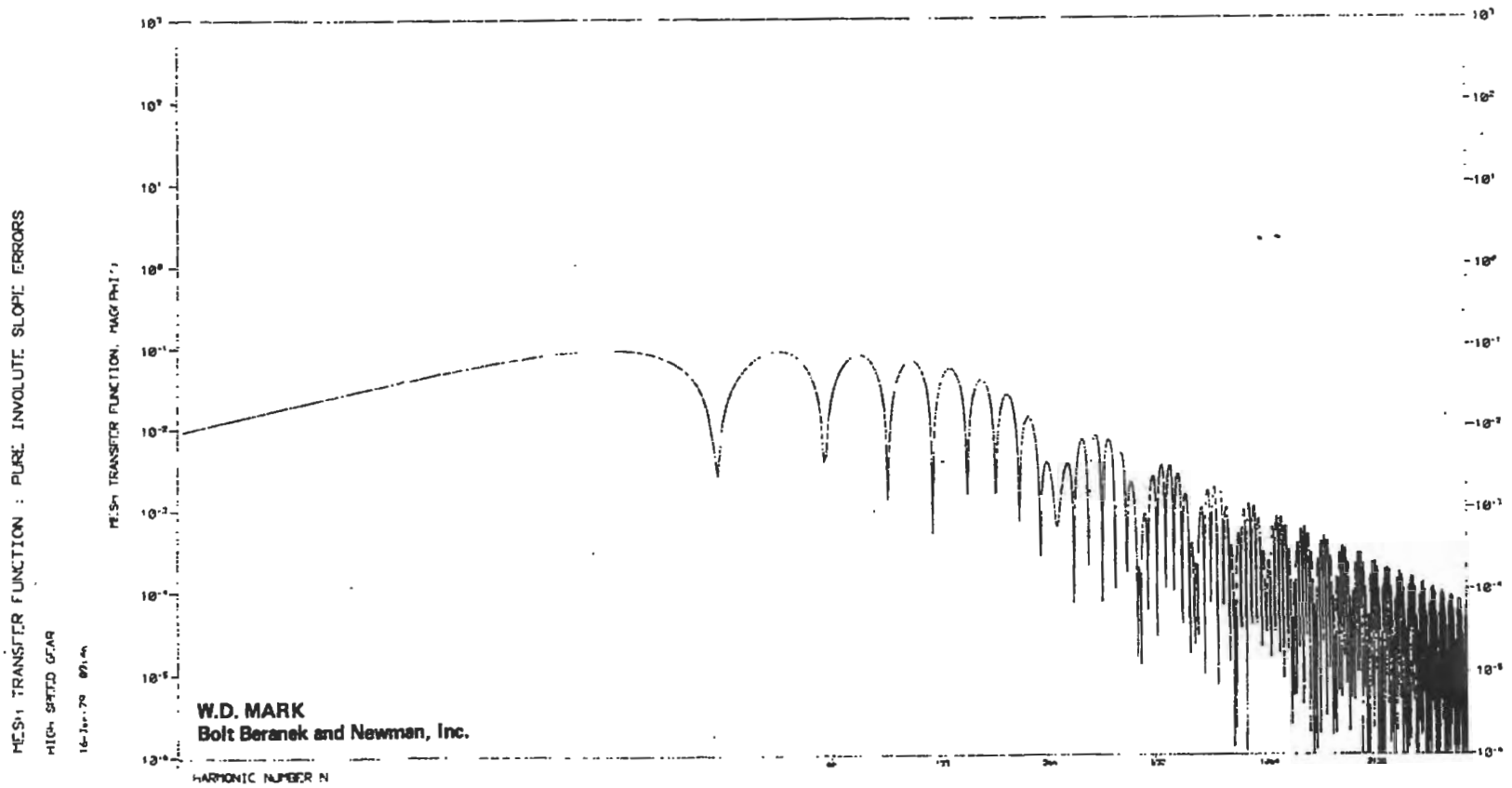

(From Presentation by W. D. Mark on 11, 12 June 1980 at NAVSSES)

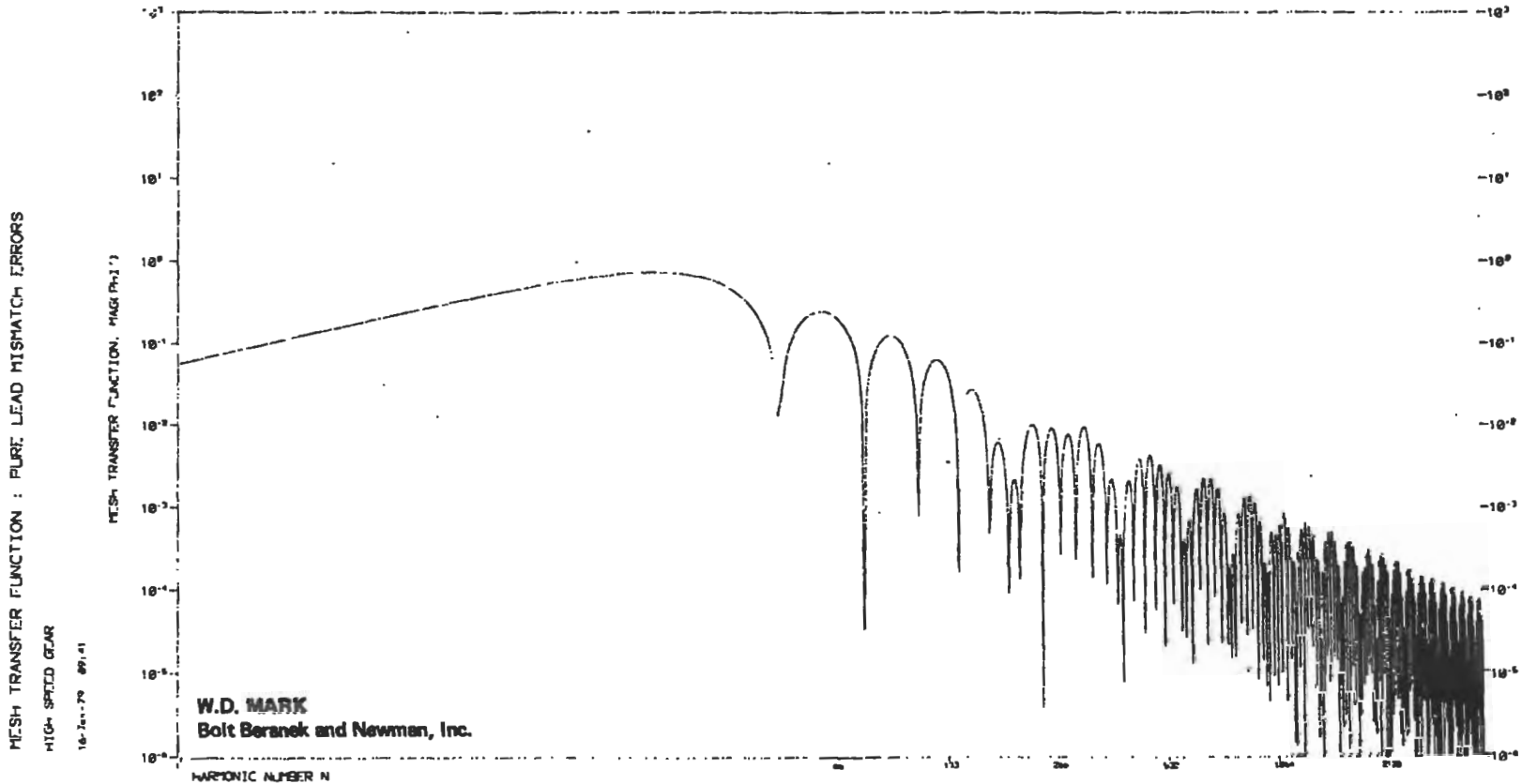

(From Presentation by W. D. Mark on 11, 12 June 1980 at NAVSSES.)

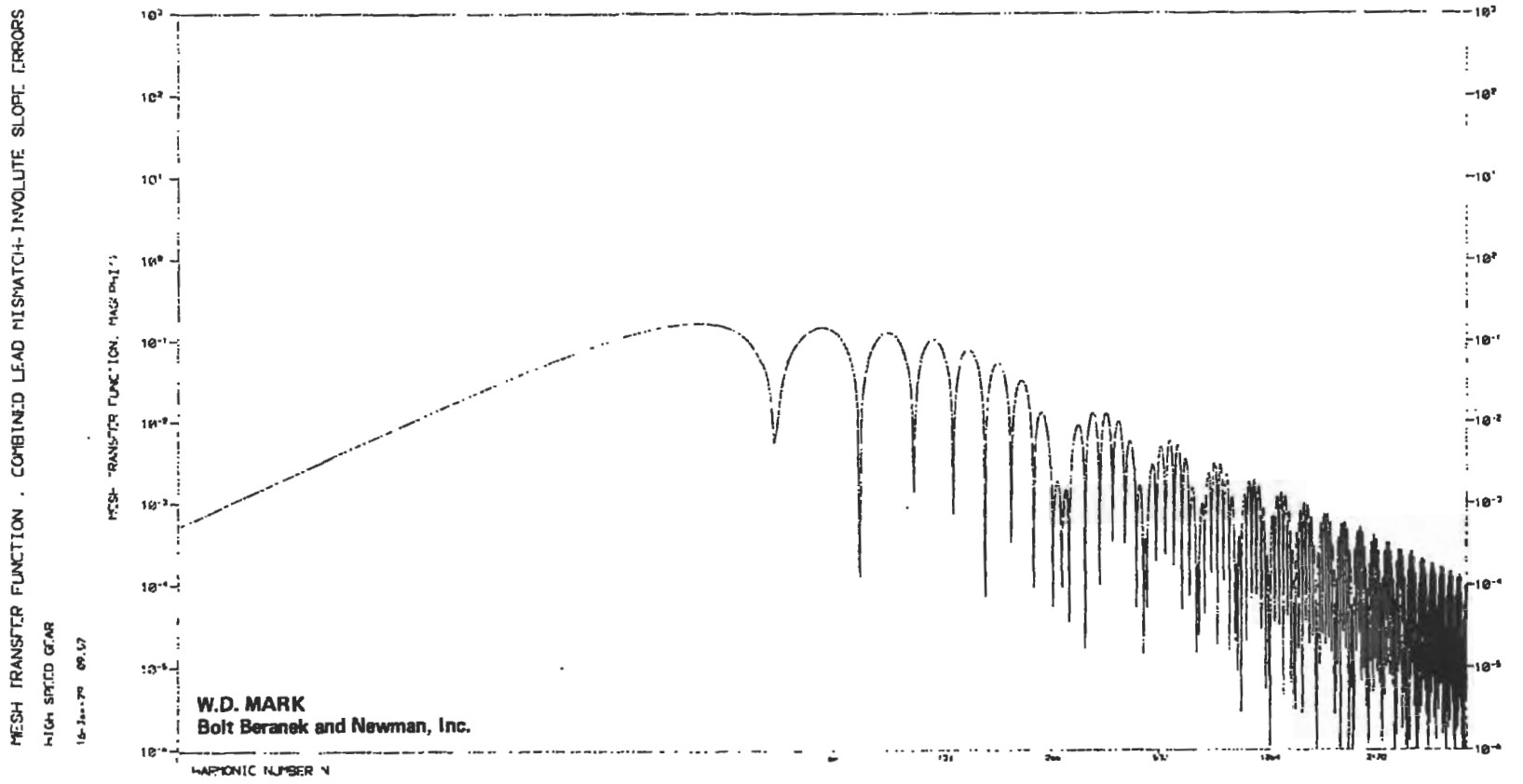

(From Presentation by W. D. Mark on 11, 12 June 1980 at NAVSSES)

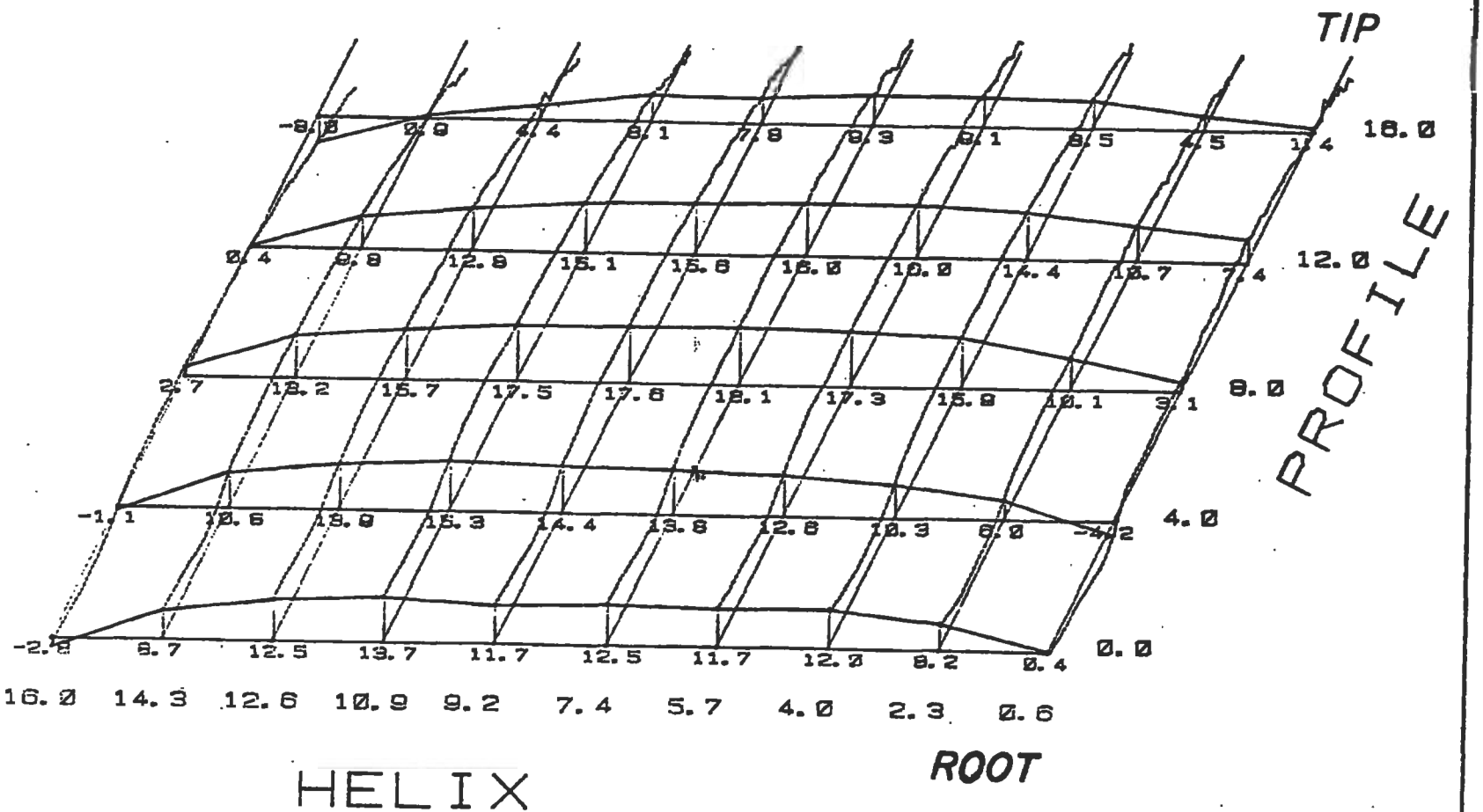

FIG. 8.

TOOTH SURFACE REPRESENTATION

HOBBED and SHAVED HIGH SPEED PINION

HELIX ANGLE VARIATION ON A GIVEN TOOTH

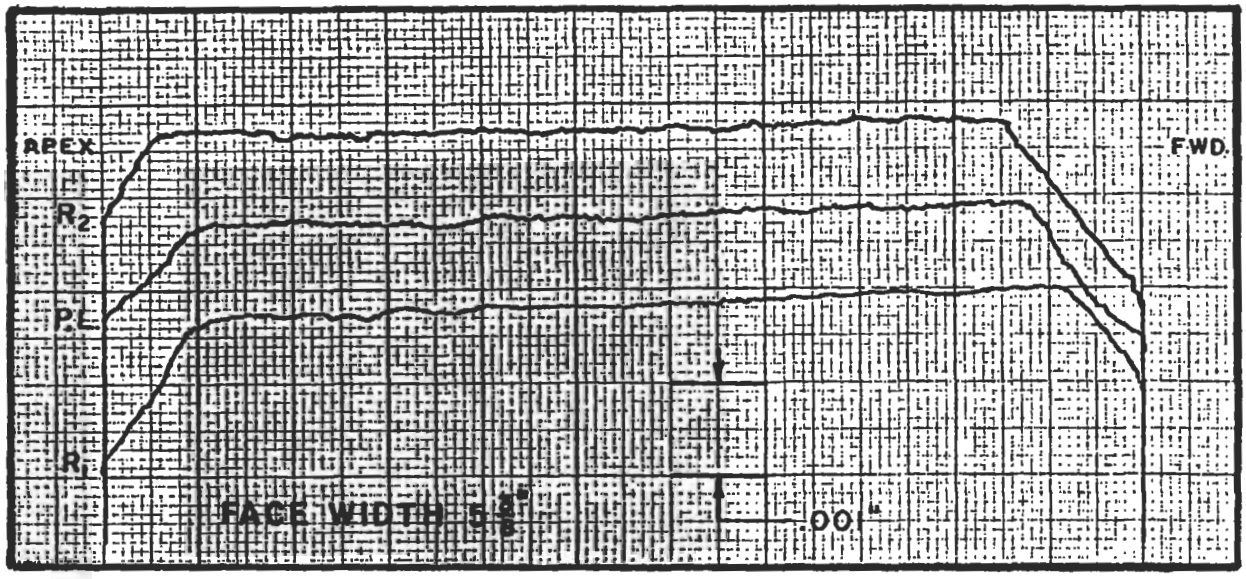

3 HELIX ANGLES AT 3 DIFFERENT DEPTHS (TOOTH No. 1)

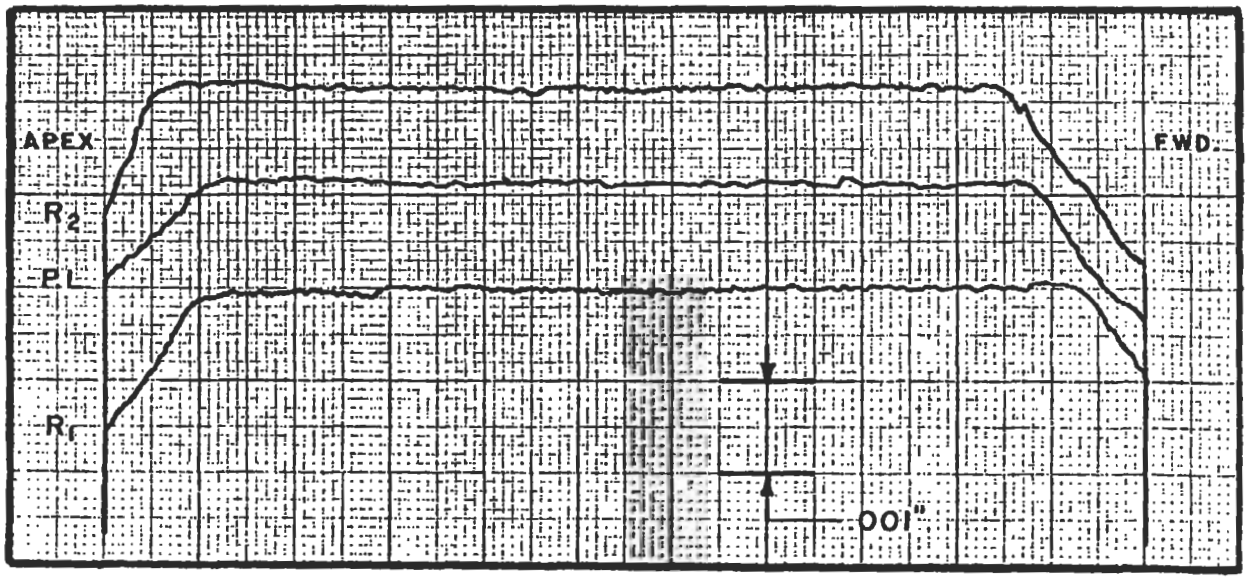

3 HELIX ANGLES AT 3 DIFFERENT DEPTHS (TOOTH No. 24)

FIG. 9.

HOBBED and SHAVED HIGH SPEED PINION

HELIX ANGLE VARIATION AROUND THE PINION
(TAKEN AT THE PITCH LINE)

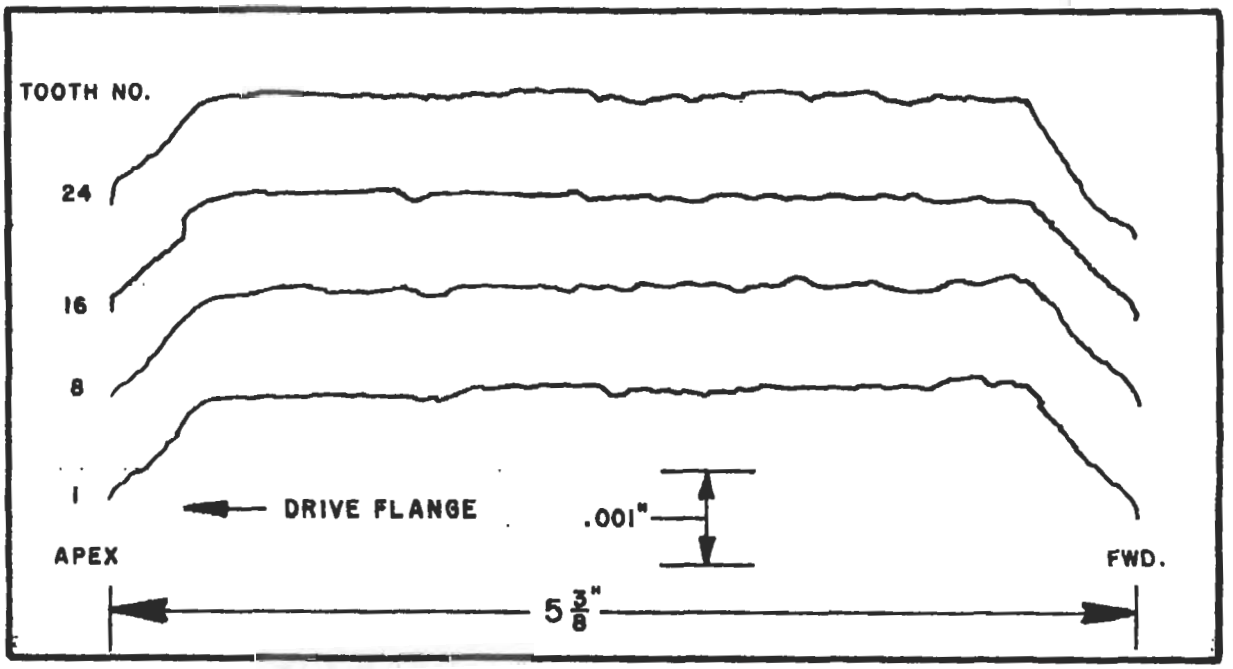

FIG. 10.

MAAG-GROUND HIGH SPEED PINION

HELIX ANGLE VARIATION ON A GIVEN TOOTH

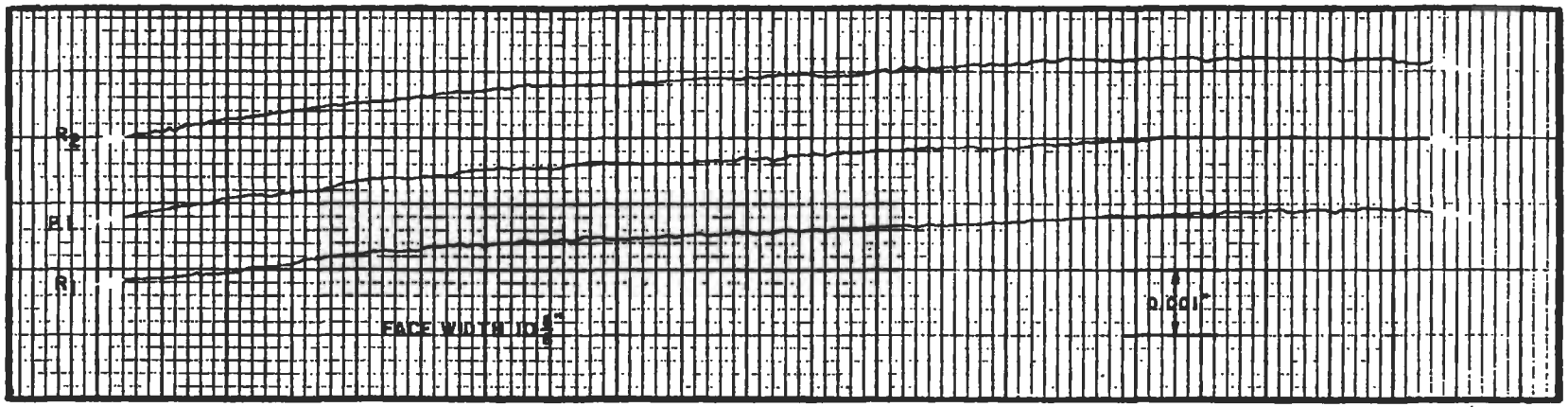

HELIX ANGLES AT 3 DIFFERENT DEPTHS (TOOTH No. 18)

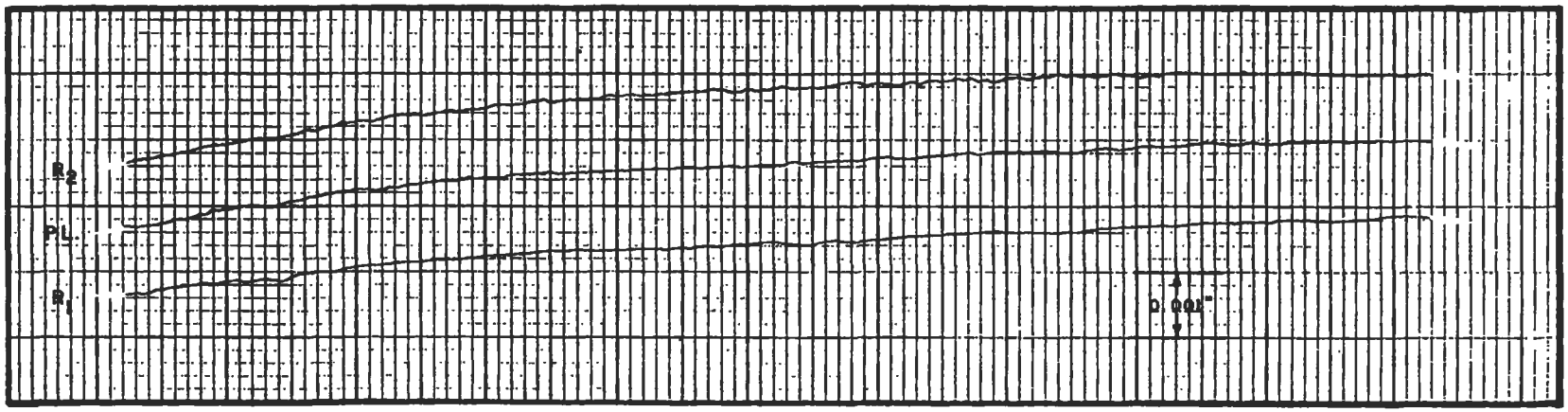

HELIX ANGLES AT 3 DIFFERENT DEPTHS (TOOTH No. 36)

FIG. 11.

MAAG-GROUND HIGH SPEED PINION

HELIX ANGLE VARIATION AROUND THE PINION

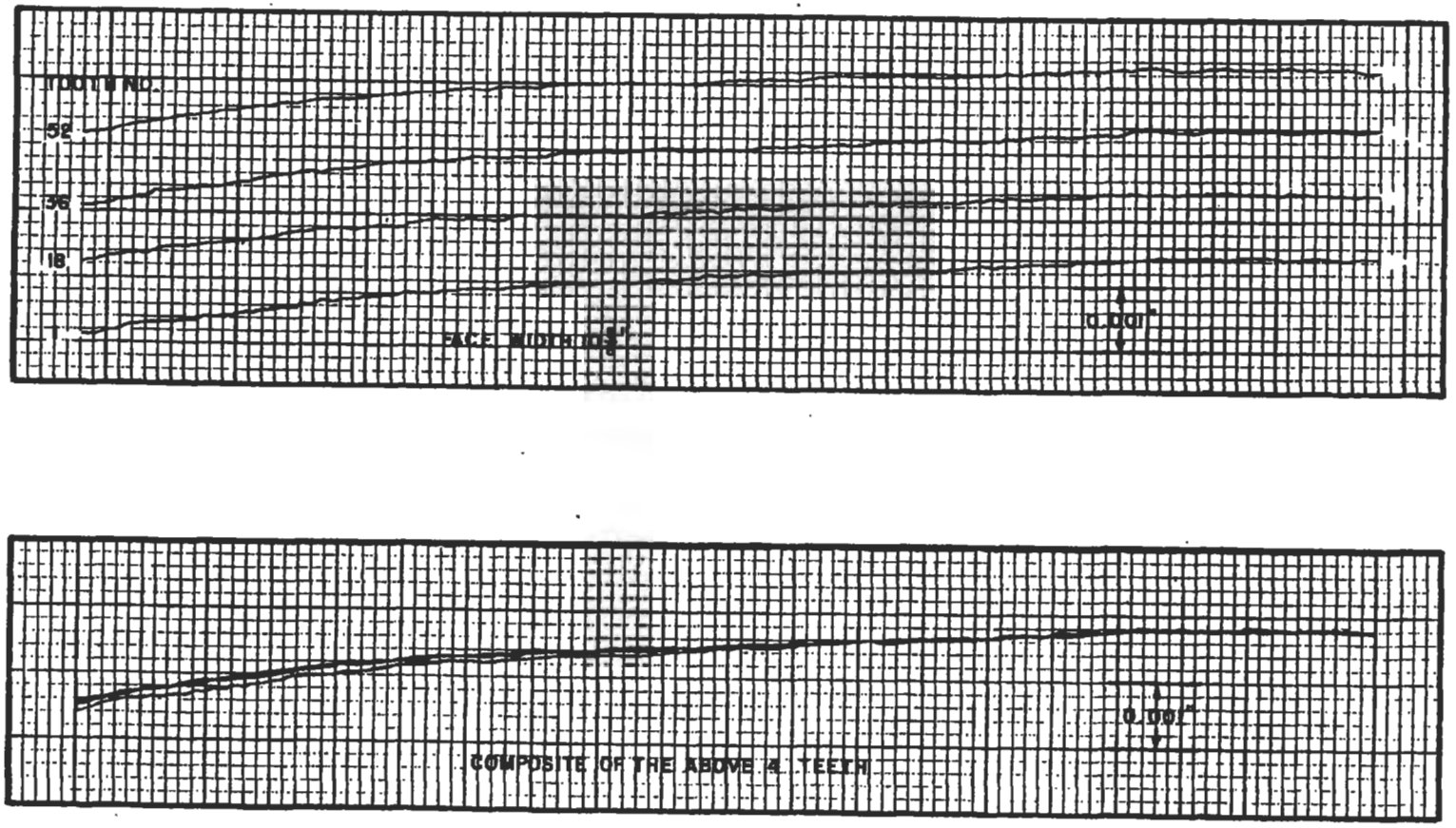

FIG. 12.

HOBBED and SHAVED HIGH SPEED PINION

PROFILE VARIATION ON A GIVEN TOOTH

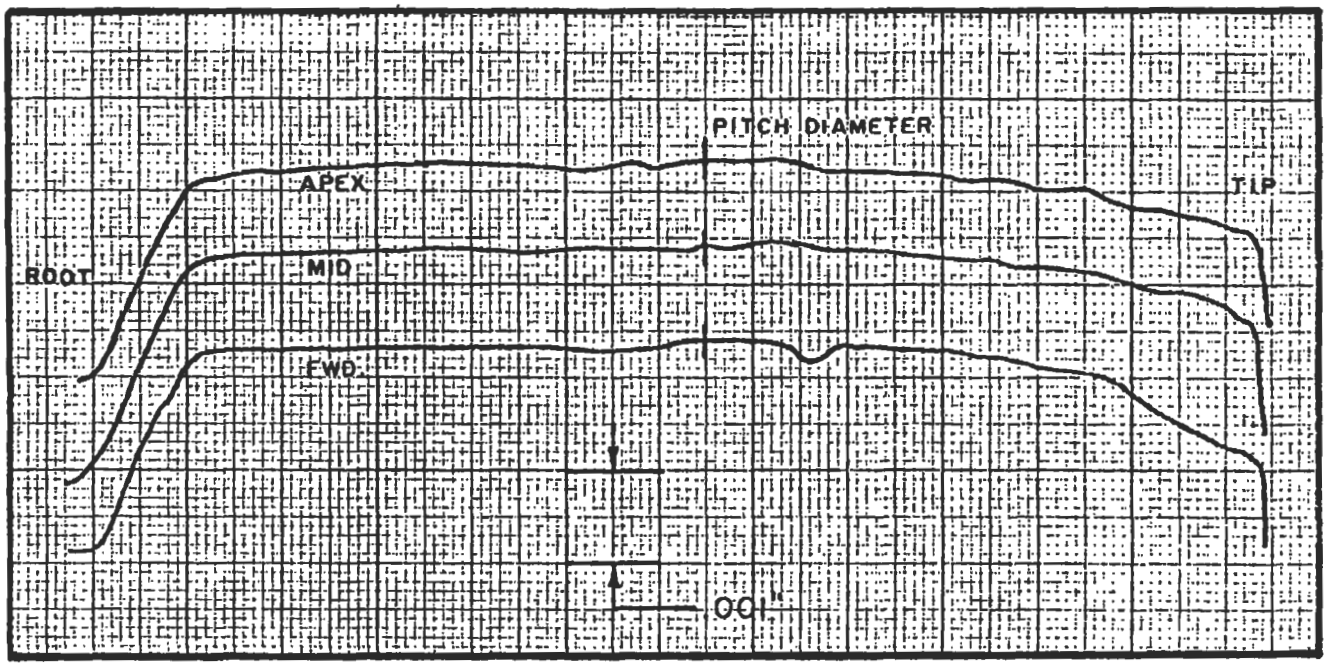

3 PROFILES AT 3 DIFFERENT LOCATIONS (TOOTH No. 1)

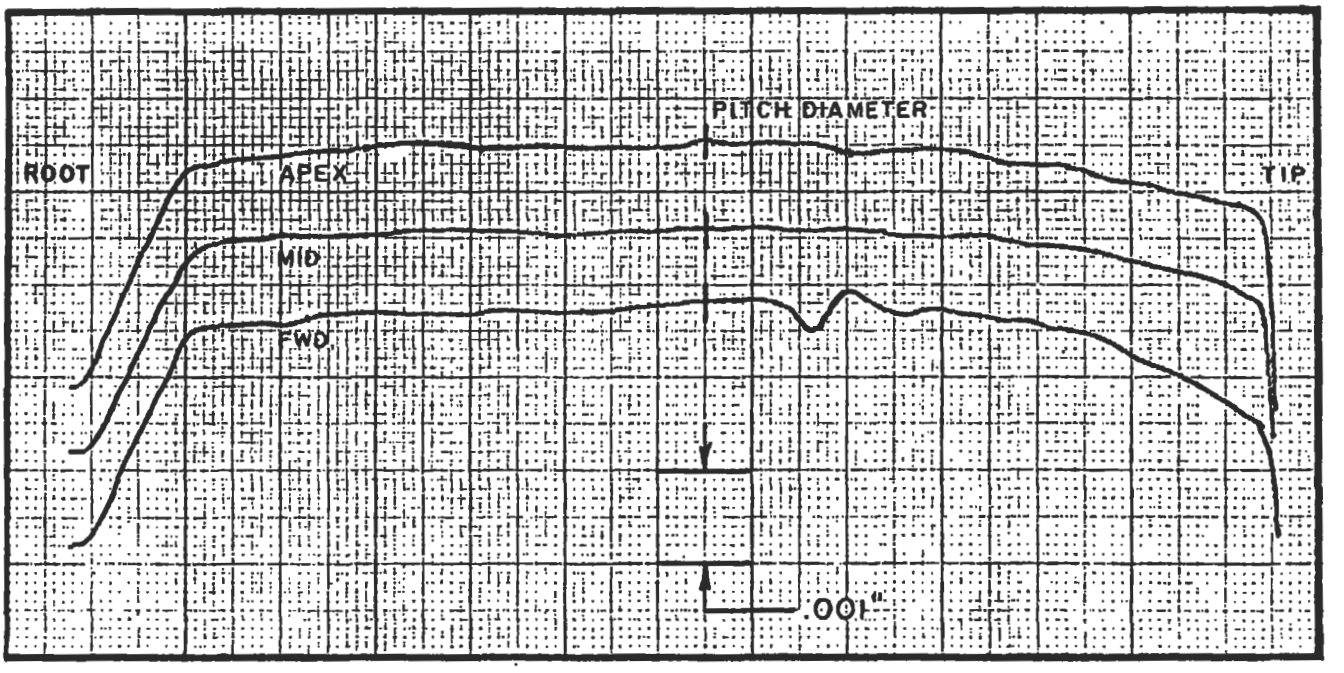

3 PROFILES AT 3 DIFFERENT LOCATIONS (TOOTH No. 8)

FIG. 13.

HOBBED and SHAVED HIGH SPEED PINION

PROFILE VARIATION AROUND THE PINION
(TAKEN AT TOOTH CENTER)

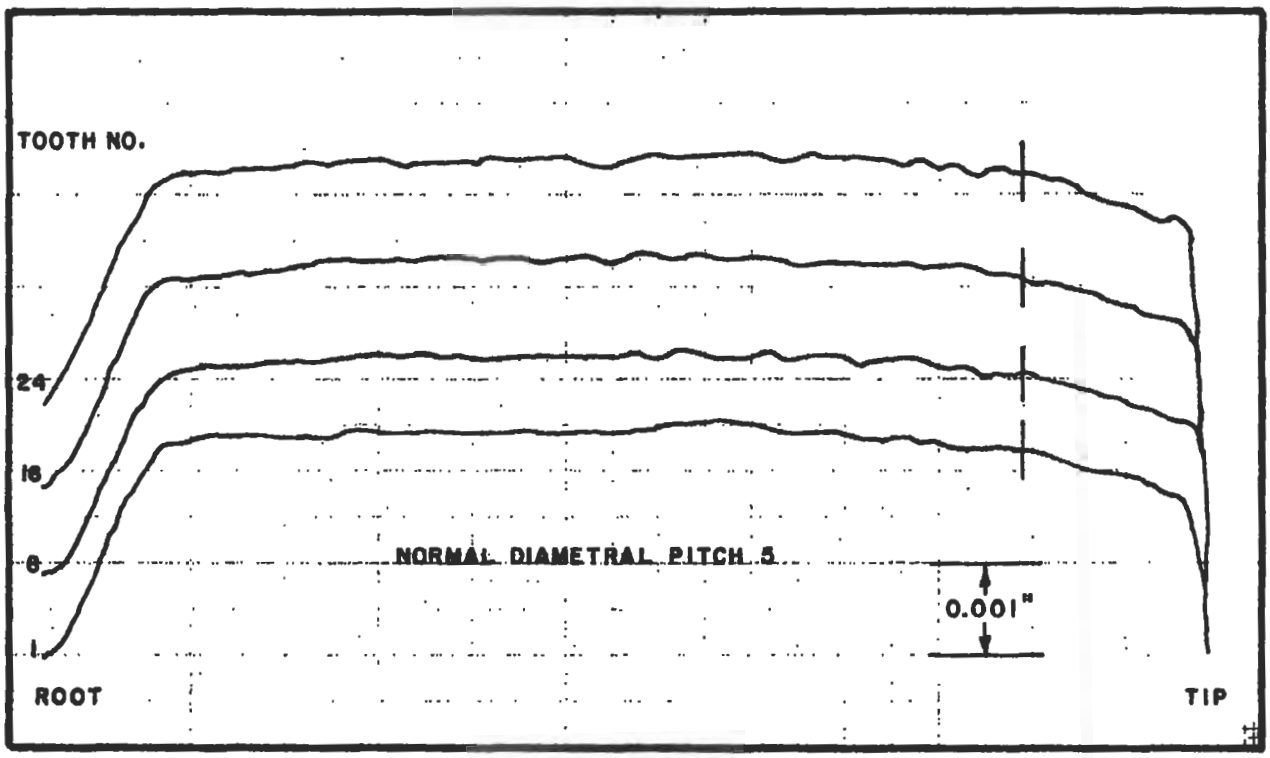

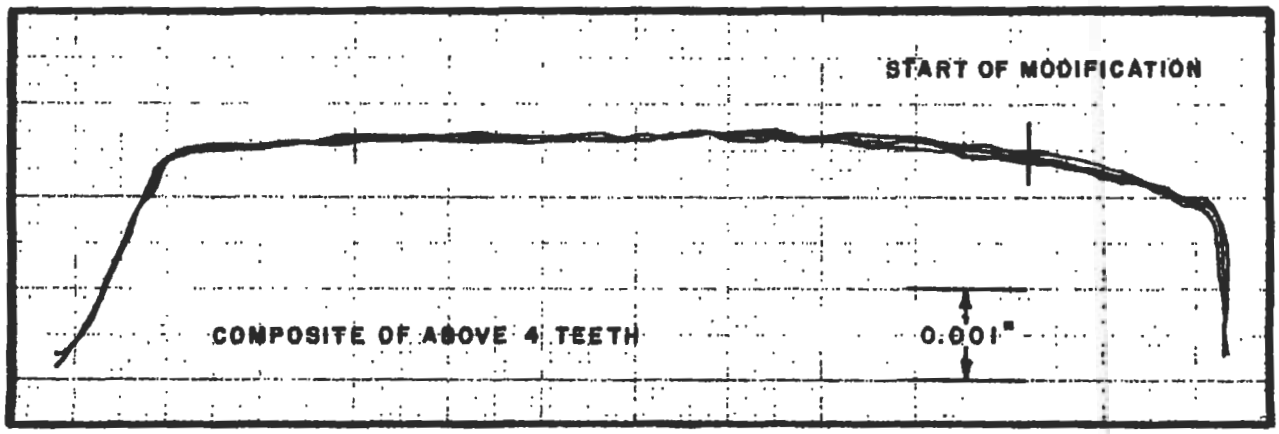

FIG. 14.

MAAG–GROUND HIGH SPEED PINION

PROFILE VARIATION ON A GIVEN TOOTH

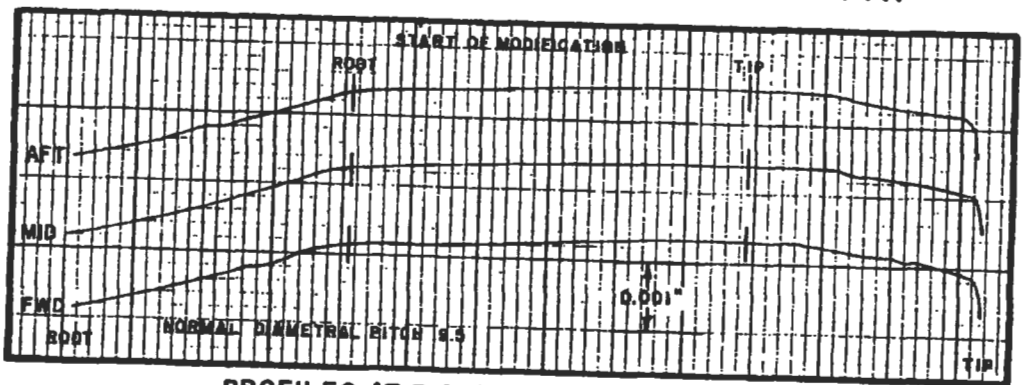

PROFILES AT 3 AXIAL LOCATIONS (TOOTH No. 1)

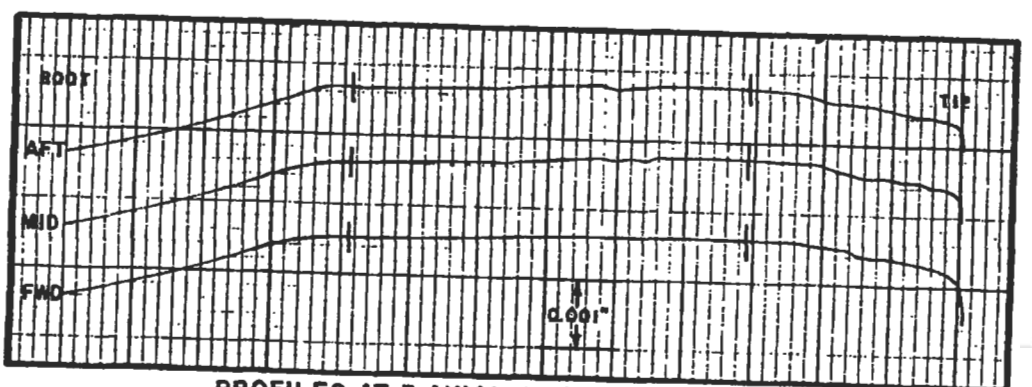

PROFILES AT 3 AXIAL LOCATIONS (TOOTH No. 36)

FIG. 15.

MAAG–GROUND HIGH SPEED PINION
PROFILE VARIATION AROUND THE PINION
(TAKEN AT TOOTH CENTER)

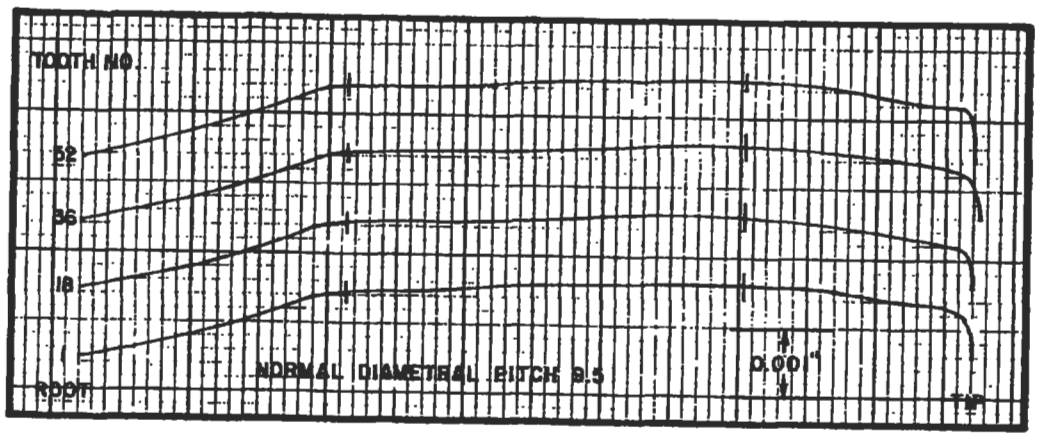

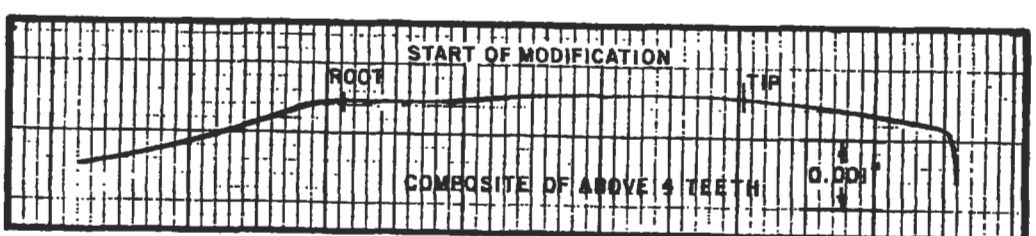

FIG. 16.

SPECTRAL DISTRIBUTION OF STRUCTUREBORNE VIBRATION TAKEN ON A REDUCTION GEAR BEARING CAP

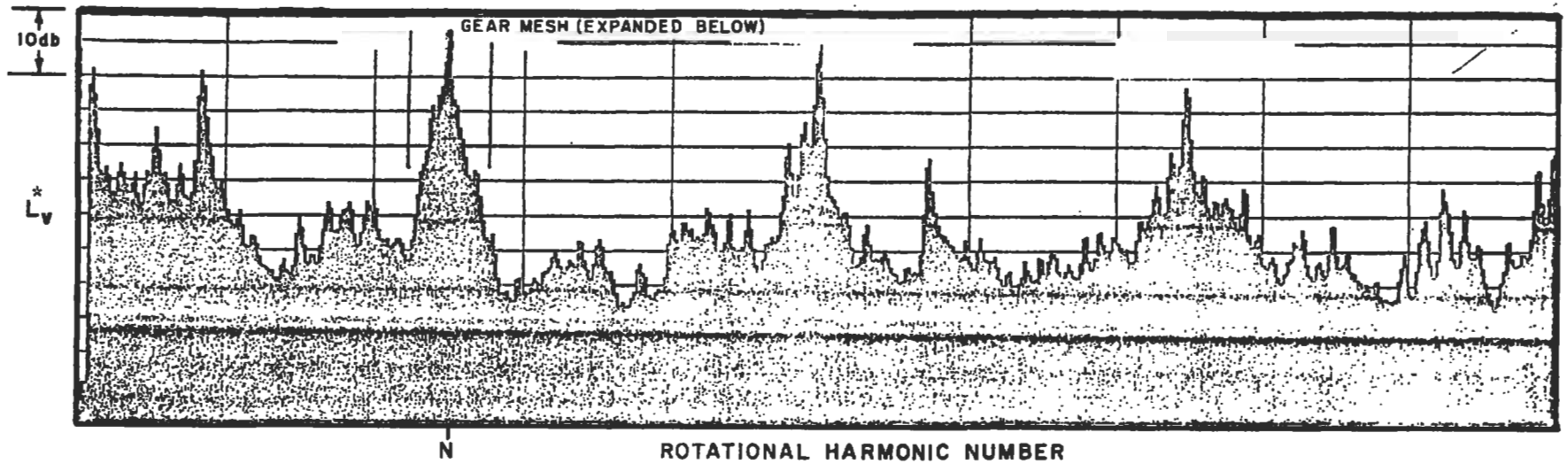

TRANSLATION AROUND GEAR MESH

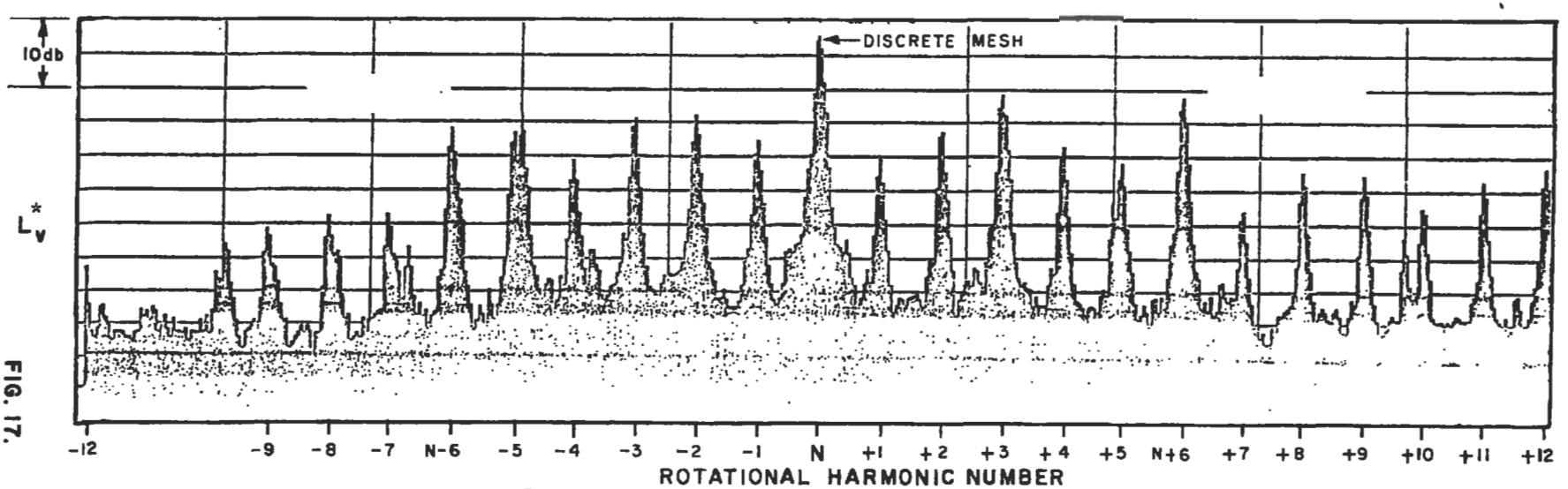

FIG. 17.

*AMPLITUDE IN VELOCITY DECIBELS re 10^{-6} cm/sec

TIME STUDY OF TRACKING FOR DISCRETE MESHING FREQUENCY
AND A PROMINENT ROTATIONAL HARMONIC (-1) VS. TEST RPM

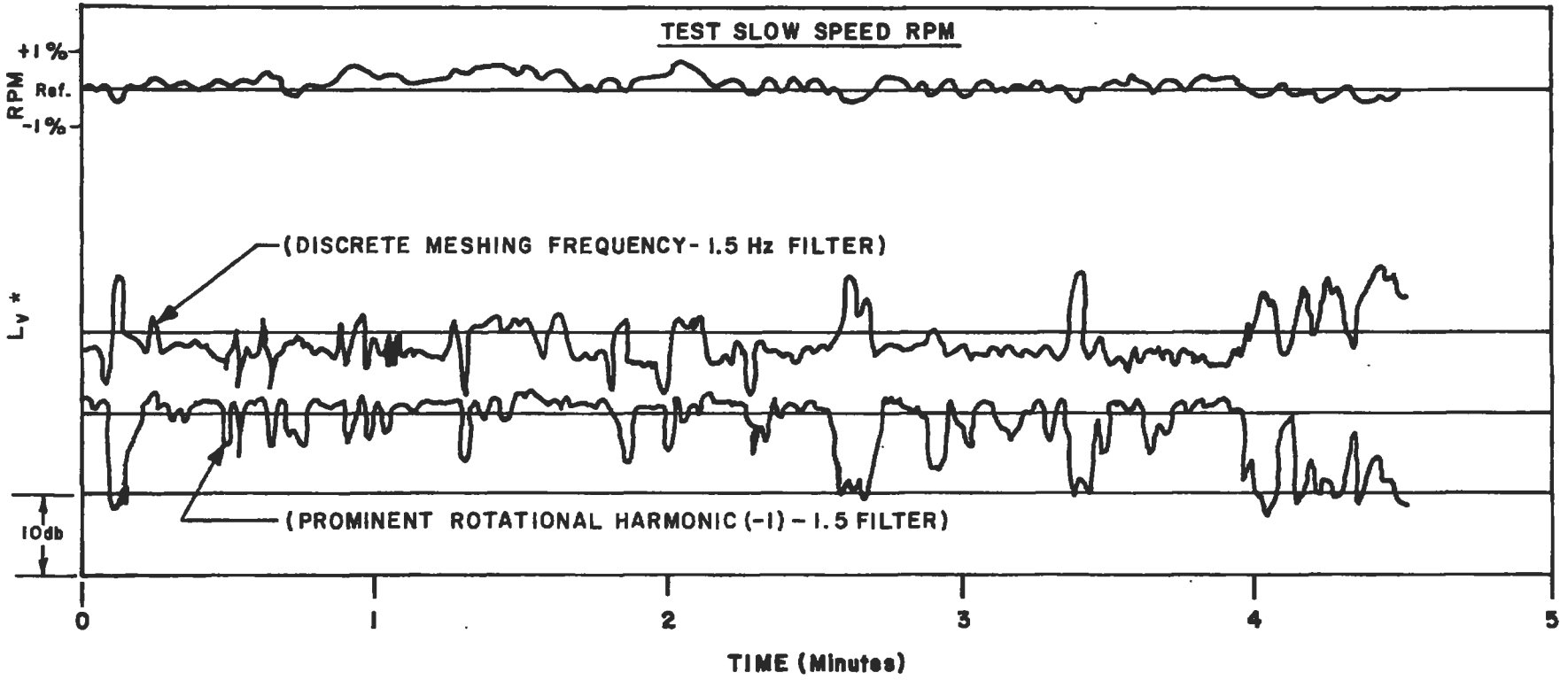

*AMPLITUDE IN VELOCITY DECIBELS re 10^{-6} cm/sec

FIG. 18.

COMPARISON OF ROTATIONAL HARMONIC STRUCTURE WITH DIFFERENT LOADS

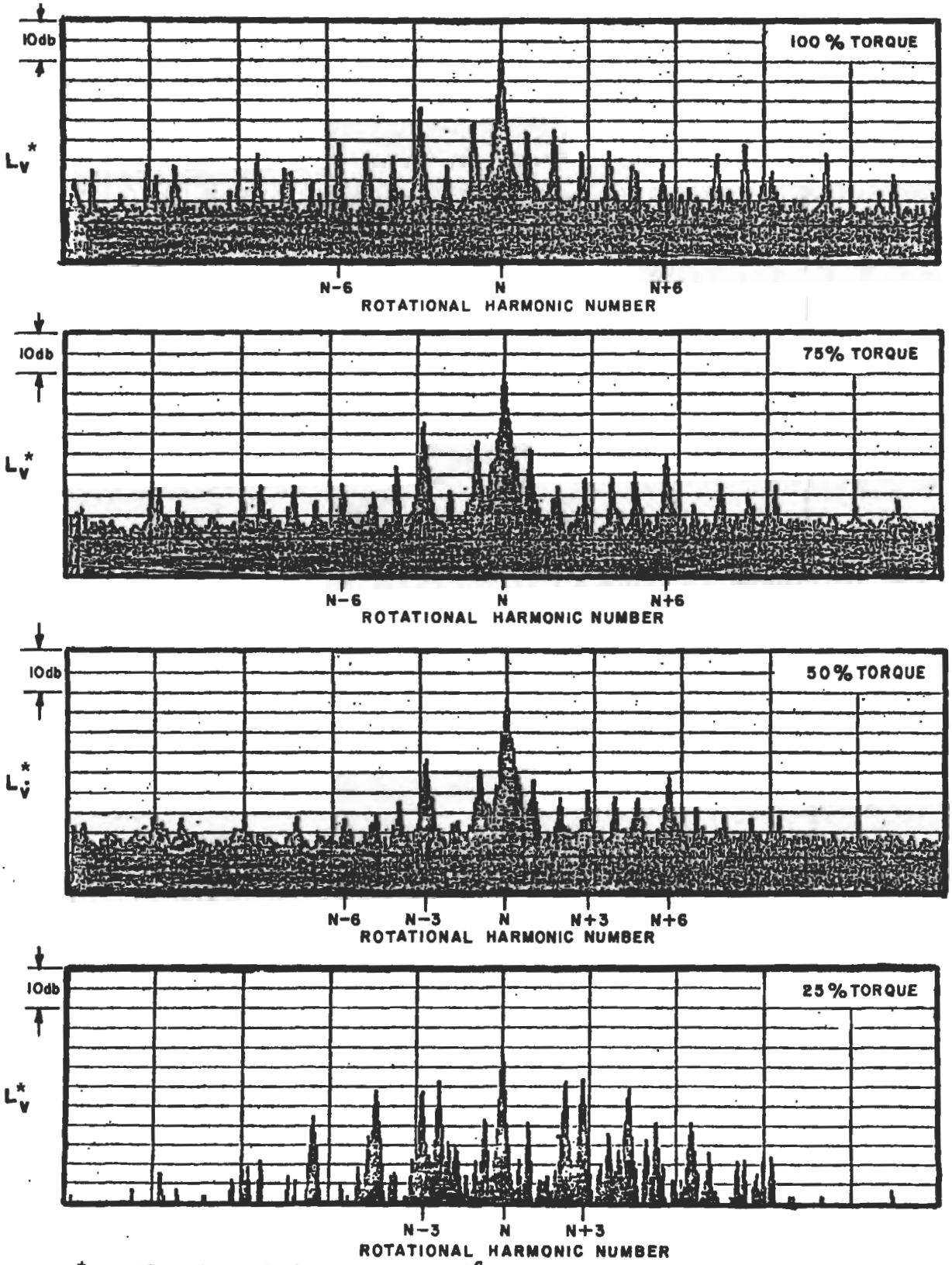

* AMPLITUDE IN VELOCITY DECIBELS re 10^{-6} cm/sec

FIG. 19.

TRANSLATED VIBRATION SPECTRUM FOR TWO "IDENTICAL" INPUT PINIONS

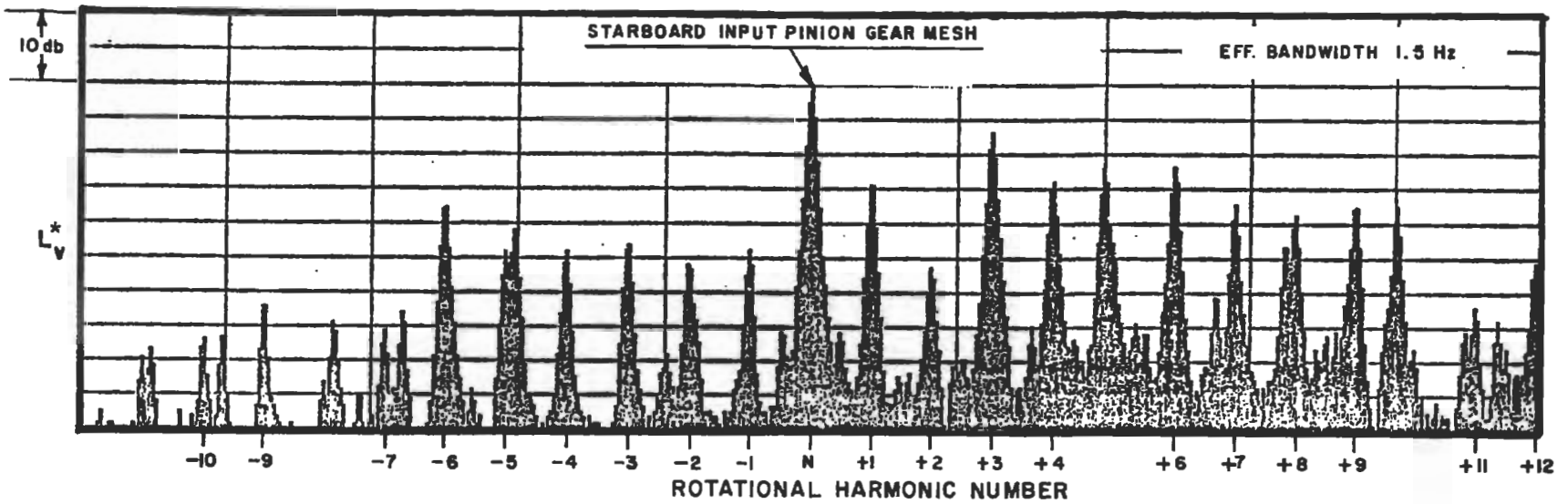

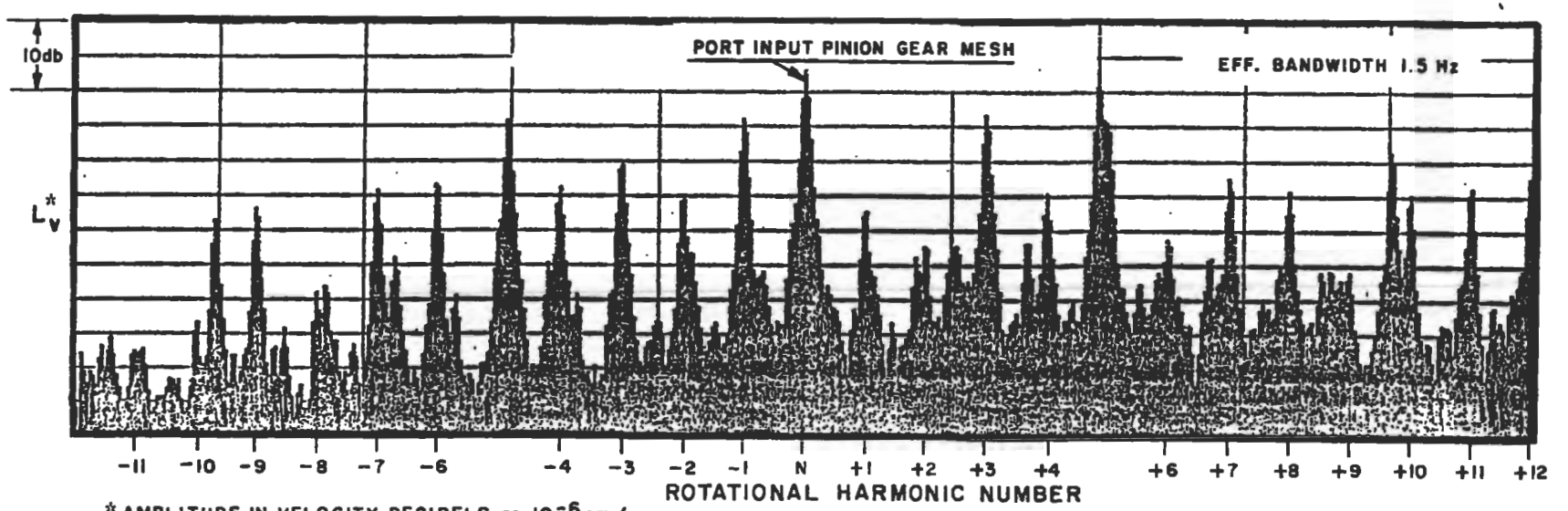

* AMPLITUDE IN VELOCITY DECIBELS re 10^{-6} cm/sec

FIG. 20.

HOBBED and SHAVED GEAR - ROTATIONAL HARMONIC STRUCTURE

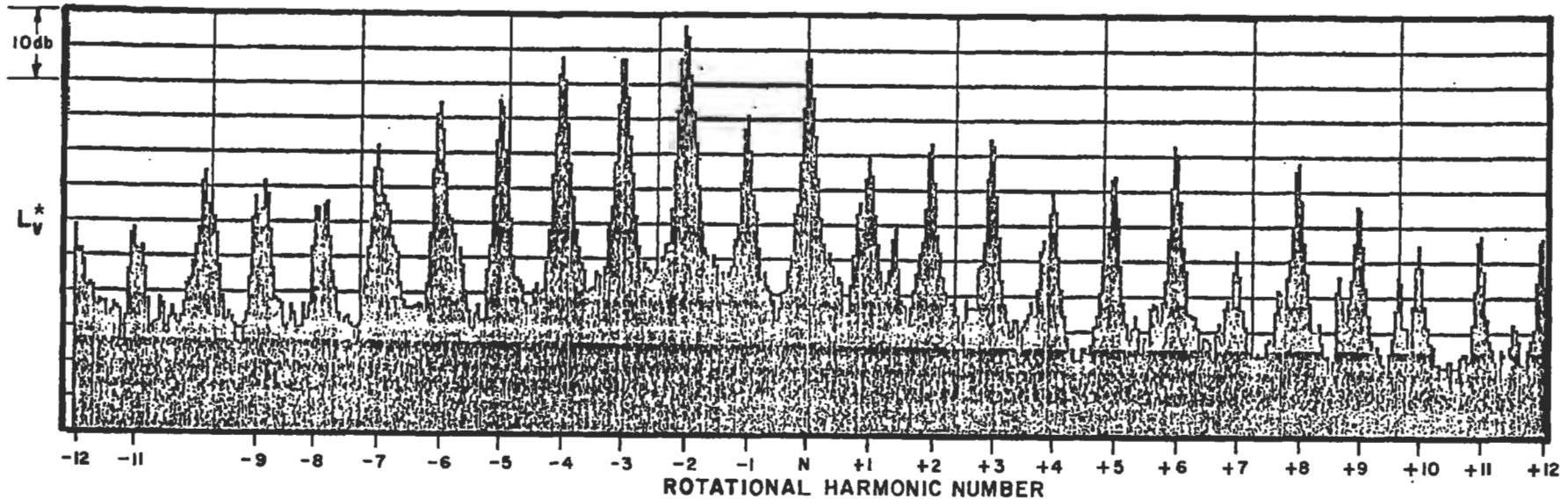

MAAG-GROUND GEAR - ROTATIONAL HARMONIC STRUCTURE

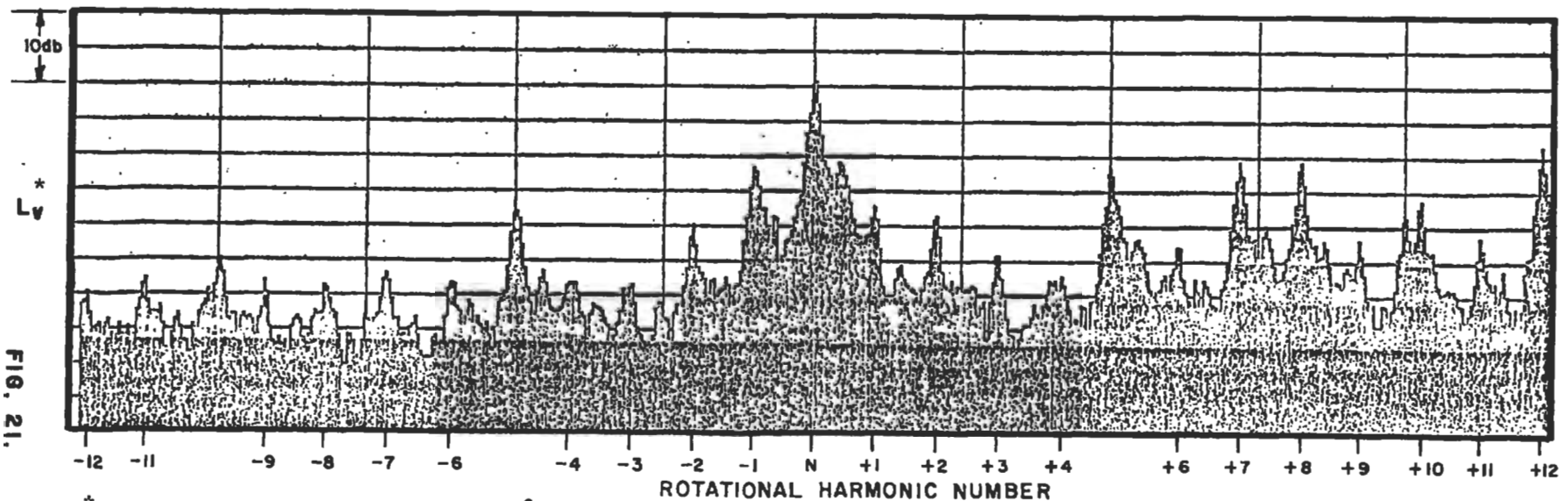

FIG. 21.

* AMPLITUDE IN VELOCITY DECIBELS re 10^{-6} cm/sec

TRANSLATED MESH FOR GEAR WITH 3 EQUALLY SPACED STIFFENERS

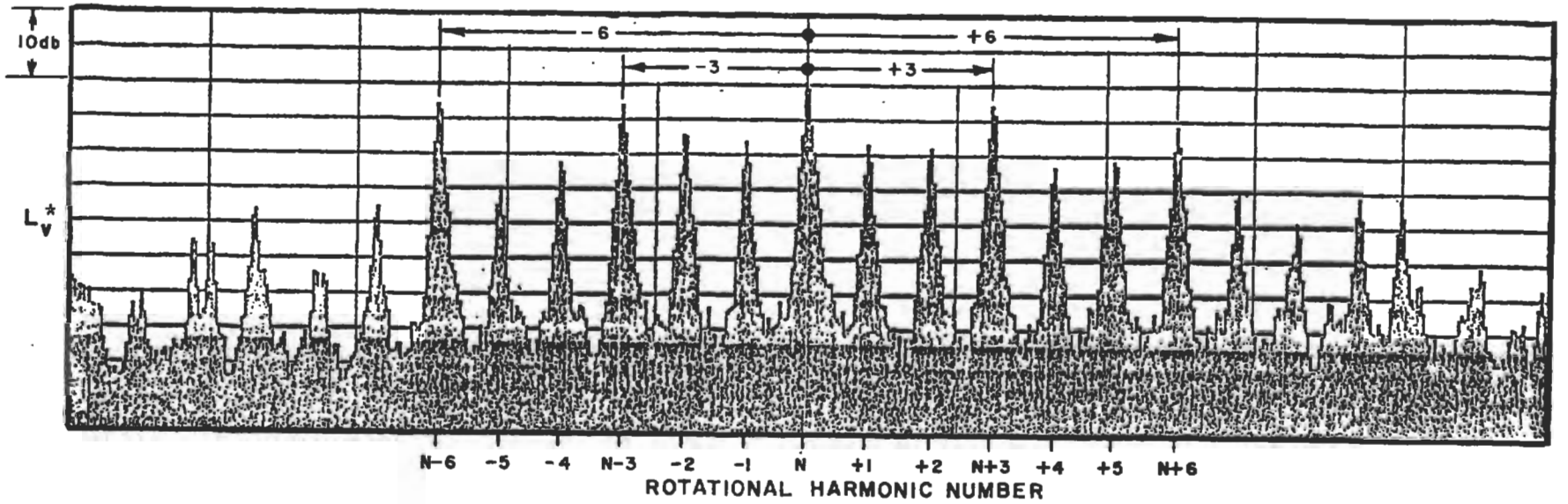

TRANSLATED MESH FOR GEAR WITH 6 EQUALLY SPACED STIFFENERS

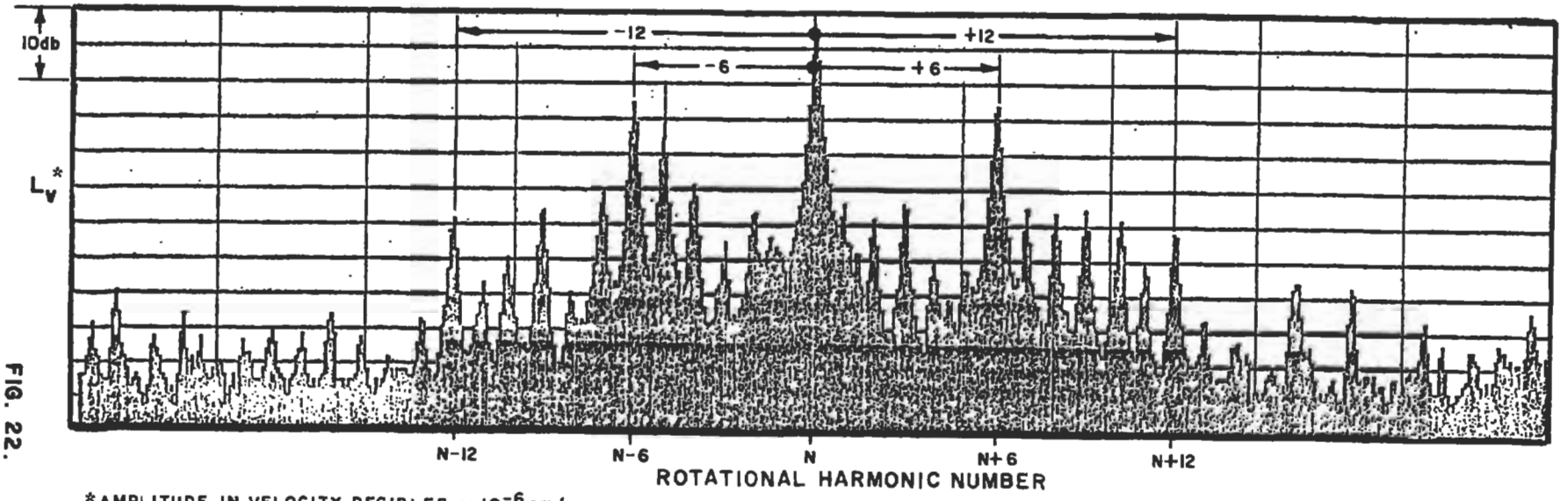

FIG. 22.

*AMPLITUDE IN VELOCITY DECIBLES re 10^{-6} cm/sec